J. Chem. Phys.

Infrared Spectroscopy of $H^+(CO)_2$ in the Gas Phase and in para-Hydrogen Matrices

Daniel Leicht,[a] Brandon M. Rittgers,[a] Gary E. Douberly,[a] J. Philipp Wagner,[a] David C. McDonald II,[a] Daniel T. Mauney,[a] Masashi Tsuge,*[bc] Yuan-Pern Lee,[bde] Michael A. Duncan*[a]

[a]Department of Chemistry, University of Georgia, Athens, GA, 30602, U.S.A.
[b]Department of Applied Chemistry, National Chiao Tung University, Hsinchu 30010, Taiwan.
[c]Institute of Low Temperature Science, Hokkaido University, Sapporo 060-0819, Japan.
[d]Center for Emergent Functional Matter Science, National Chiao Tung University, Hsinchu 30010, Taiwan.
[e]Institute of Atomic and Molecular Sciences Academia Sinica, Taipei 10617, Taiwan.

*Email: tsuge@lowtem.hokudai.ac.jp (MT), maduncan@uga.edu (MAD)

Abstract

The $H^+(CO)_2$ and $D^+(CO)_2$ molecular ions were investigated with infrared spectroscopy in the gas phase and in *para*-hydrogen matrices. In the gas phase, ions were generated in a supersonic molecular beam by a pulsed electrical discharge. After extraction into a time-of-flight mass spectrometer, the ions were mass selected and probed with infrared laser photodissociation (IR-PD) spectroscopy in the 700–3500 cm^{-1} region. Spectra were measured using either argon or neon tagging, as well as tagging with an excess CO molecule. In solid *para*-hydrogen, ions were generated by electron bombardment of a mixture of CO and hydrogen and absorption spectra were recorded in the 400–4000 cm^{-1} region with a Fourier-transform infrared spectrometer. Comparison of measured spectra with the predictions of anharmonic

theory at the CCSD(T)/ANO1 level suggests that the predominant isomers formed by either argon tagging or *para*-hydrogen isolation is a higher lying (+7.8 kcal mol^{-1}), less symmetric isomer, and not the global minimum proton-bound dimer. Changing the formation environment or tagging strategy produces other non-centrosymmetric structures, but there is no spectroscopic evidence for the centrosymmetric proton-bound dimer. The formation of higher energy isomers may be caused by a kinetic effect, such as the binding of X (= Ar, Ne or H_2) to $H^+(CO)$ prior to the formation of X $H^+(CO)_2$. Regardless, there is a strong tendency to produce non-centrosymmetric structures in which HCO^+ remains an intact core ion.

I. Introduction

The formyl cation (HCO^+) is one of the most abundant molecular ions in interstellar space.[1-12] HCO^+ was suggested by Herbst and Klemperer to be formed early in a sequence of reactions leading to complex molecular species and thus is an important reactive intermediate in interstellar chemistry.[1] Its formation in diffuse clouds is believed to be due to the reaction of C^+ with CO and H_2 or that of C^+ with H_2 and atomic oxygen. In dense clouds, on the other hand, a reaction of H_3^+ with molecular CO produces HCO^+. In both environments, the primary ion is formed by radiation-induced ionization. Its high abundance and large dipole moment make the formyl cation a valuable tracer in the interstellar medium. Carbon monoxide is ubiquitous in space and the most abundant molecular species after H_2. Therefore, the $HCO^+(CO)$ complex has also been suggested to form in dense molecular clouds.[11,12] Unfortunately, there is no spectroscopy on this fascinating ion. In this paper, we measure infrared spectra and compare them to computational predictions to explore the structure of the $H^+(CO)_2$ ion.

HCO^+ was first detected in space in 1970 by Buhl and Snyder, who called it "X-ogen," as they could not assign the observed microwave band at 89.190 GHz to any known molecular species.[13] Soon after this, Klemperer suggested that this line originates from HCO^+.[14,15] In 1975, the assignment was confirmed in laboratory experiments by Woods *et al*.[16] After its initial detection, formyl cation was found in multiple interstellar sources and its microwave spectrum was studied extensively.[16-20] The first infrared studies on HCO^+ were carried out between 1983 and 1987, in which the frequencies of 3088.7, 829.7, and 2183.9 cm^{-1} were reported for the υ_1 (C–H stretch), υ_2 (bend), and υ_3 (C–O stretch) bands, respectively.[21-26] Infrared spectroscopy has also been reported for the HOC^+ isomer.[27] Recently, a theoretical study has been published in which spectroscopic parameters were derived for all isotopologues of HCO^+ and HOC^+ using full-dimensional rovibrational calculations.[28]

Weakly bound complexes of HCO^+ have been investigated using mass spectrometry, laser photodissociation spectroscopy, and theory.[29-35] Bieske *et al.* investigated the molecular complex of HCO^+ and H_2,[29] whereas Nizkorodov *et al.* studied HCO^+Ar_n and HCO^+Ne_n complexes.[30-32] More recently, Schlemmer and coworkers reported a spectrum for HCO^+He.[33] Bieske *et al.* determined a planar T-shaped structure for $HCO^+(H_2)$ with no significant distortion on either of the two sub-units.[29] They observed six vibrational transitions at 2840, 2876.36, 2879.08, 3145, 4060.315, and 4063.822 cm^{-1}, three of which were combination bands. Nizkorodov *et al.* investigated the influence of the HCO^+Ar_n cluster size (for n = 1–13) on the υ_1 band.[30] By analyzing the daughter ion yields, they were able to extract argon binding energies from the branching ratios. These binding energies, together with vibrational band shifts, revealed the formation of the primary and secondary solvation shells for argon around the linear $Ar\text{-}HCO^+$ core ion.

Proton-bound dimers (PBDs) are important intermediates in proton transfer reactions, which play crucial roles in many biological systems, in acid-base chemistry, in chemical ionization mass spectrometry, and in interstellar chemistry.[36-45] A proton-bound dimer $A\text{-}H^+\text{-}B$ can be understood as an intermediate in the proton transfer from species AH^+ to species B. Many studies have been carried out on homogeneous as well as mixed PBDs in mass spectrometry.[39-45] Ion and cluster-ion spectroscopy has also been applied to many of these systems.[46-74] Our groups have studied the protonated water dimer,[47,62,63,68] the $H^+(N_2)_2$ cation,[60,74] the H_5^+ cation,[61,64,71] the protonated argon dimer,[66] protonated xenon or krypton or mixed dimer,[72] protonated carbon dioxide dimer,[58,73] protonated acetone dimer,[57] protonated acetylene dimer,[59] protonated water-benzene clusters,[65] protonated formaldehyde dimer,[67] protonated O_2 dimer,[70] and protonated ethylenediamine dimer.[68] Prominent features in the infrared spectroscopy of such proton-bound dimers are the shared proton vibrations, which occur

both parallel to the molecular axis (which is the proton transfer coordinate) and perpendicular to it. Because of the charge in motion, these vibrations have strong infrared intensities. Because of the nuances in proton binding in different systems, the potential energy surface along these vibrations are highly variable, providing a severe challenge to description by harmonic vibrational theory. Johnson and coworkers have studied these vibrations for a series of RO-H^+-OR' complexes, finding a strong correlation with the proton affinity differences (ΔPA) between the two binding partners.[53] Symmetric PBDs were found to have shared proton vibrations near 1000 cm^{-1}, whereas asymmetric complexes with high ΔPA values had much higher shared-proton vibrational frequencies, approaching the free-OH stretches in some cases. In other examples of symmetric PBD systems, the shared proton stretch has been found to have much lower frequencies (e.g., 743 cm^{-1} for N_2-H^+-N_2; 379 cm^{-1} for H_2-H^+-H_2).[60,64,71]

The $H^+(CO)_2$ ion has been produced and studied in mass spectrometry, where a bond energy of 10.8 kcal/mol was obtained for the association reaction $H^+CO + CO$.[75,76] A series of computational studies including anharmonic vibrational interactions have focused on the $H^+(CO)_2$ dimers and the analogous $H^+(N_2)_2$ species.[74,77-84] In contrast to the centrosymmetric ($D_{\infty h}$) structure of $H^+(N_2)_2$, it was found that $H^+(CO)_2$ forms a linear PBD, but one which is non-centrosymmetric ($C_{\infty v}$).[79,81,84] A binding energy of 4634 cm^{-1} (13.2 kcal/mol) was reported,[81] in reasonable agreement with previous estimates. The study by Terrill and Nesbitt[81] as well as one by Fortenberry *et al.*[84] investigated the vibrational spectrum of $H^+(CO)_2$. Terrill and Nesbitt[81] focused on the symmetric and asymmetric proton stretch vibrations and their overtones and combinations. They found a barrier to proton transfer of 398 cm^{-1}, and a zero-point energy comparable to this. Fundamental frequencies of 298 and 386 cm^{-1} were obtained, but no vibrations with significant intensity were reported above 1000 cm^{-1}. Fortenberry *et al.* also included higher frequency vibrations from other modes such as the carbonyl stretch.[84] They

reported a binding energy of 4283 cm^{-1} (12.2 kcal/mol) and a barrier at the centrosymmetric structure of 394 cm^{-1}. They also concluded that the zero-point energy is comparable to the barrier height, and that dynamic effects should yield a centrosymmetric structure. They calculated transition frequencies using vibrational self-consistent field and vibrational configuration interaction methods. Using 4- and 5-mode representations, they predicted bands at 2308.2 (0), 2246.3 (54), 272.3 (0), 1184.9 (8), 285.4 (0), 316.5 (5186), and 148.1 (16) cm^{-1} for the υ_1 through υ_7 vibrations, respectively (IR intensities, km/mol, in parentheses). The perpendicular (υ_4 1184.9 cm^{-1}) and parallel (υ_6 316.5 cm^{-1}) proton stretch vibrations were predicted to have frequencies deviating significantly from harmonic values. Unfortunately, no spectroscopic study on $H^+(CO)_2$ has yet been reported to test these predictions.

In the present study, we report the first experimental infrared spectroscopy on $H^+(CO)_2$ and $D^+(CO)_2$. We employ infrared photodissociation (IR-PD) spectroscopy of mass-selected ions in the gas phase, which has the advantage of mass selection, but the disadvantage that band intensities may be affected by the photodissociation efficiency. We also employ *para*-hydrogen (*p*-H_2) matrix isolation infrared spectroscopy, which lacks mass selection, but should measure true absorption strengths and covers a wider range of infrared frequencies. Comparing the spectra from both methods with the results of quantum-chemical calculations, we find the structure for $H^+(CO)_2$ to be either a non-linear species, or a linear non-centrosymmetric species, neither of which is expected on the basis of previous theoretical work.

II. Methods

A. Experimental

In the gas phase experiments, formyl cations were produced in a pulsed electrical discharge in a supersonic expansion using methods described previously.[85] Mixtures of 1–5%

H_2 or D_2 and CO in argon, neon, or pure CO were used as expansion gases in different experiments. After its formation, the molecular beam was skimmed into a second chamber, where ions were pulse-extracted into a reflectron time-of-flight mass spectrometer.[86] A pulsed deflection plate was used to mass select the ions of interest. At the turning point of the reflectron, the ion packet was irradiated with the tunable infrared output of a Nd:YAG pumped OPO/OPA system (LaserVision). Because infrared excitation is not energetic enough to dissociate $H^+(CO)_2$, we employed the method of "tagging" with weakly-bound rare gas atoms such as argon or neon.[87-103] Therefore, the experimental spectra were recorded by producing a tagged ion such as $H^+(CO)_2Ar$ and monitoring the loss of argon as a function of the infrared photon energy. Spectral intensities were not corrected for laser power because of variation in spot size/shape of the laser across the spectrum and the resulting change in ion beam/laser overlap.

The experimental setup used for *p*-H_2 matrix isolation experiments was described in detail elsewhere.[101-103] Mixtures of CO/*p*-H_2 (1/10000, 1/2000, 1/1000, or 1/700) were bombarded with electrons during deposition at 3.2 K for 7–8.5 hours and infrared spectra were recorded with a Fourier-transform infrared spectrometer (Bruker, Vertex 80v) equipped with a KBr beam splitter and a Hg-Cd-Te detector. The deposited matrix was then kept in darkness for a prolonged period to allow diffusion of solvated electrons. These electrons are expected to neutralize protonated species so that the intensities of lines associated with the protonated species decrease during this period. Similar to the IR-PD experiments, deuteration experiments used a deposit of CO/*n*-D_2. Because electron diffusion is limited in a deuterium matrix, the electron-bombarded matrix was irradiated with light at 365 nm from a light-emitting diode to mobilize trapped electrons. Secondary photolysis was performed with light at 254 nm from a low-pressure mercury lamp.

B. Computational

Density functional theory and ab initio calculations were carried out using the Gaussian09[107] and CFOUR[108] program packages. Geometries of $H^+(CO)_2$, $H^+(CO)_2Ar$, $H^+(CO)_2Ne$, or $H^+(CO)_3$ and their deuterated isotopologues were pre-optimized using the B3LYP/aug-cc-pVTZ level of theory. Further geometry optimizations and anharmonic frequency calculations using second-order vibrational perturbation theory (VPT2) were performed at the CCSD(T)/ANO1 level of theory.

III. Results and Discussion

A. Infrared photodissociation (IR-PD) experiments

In an argon expansion seeded with hydrogen and CO, the pulsed discharge/supersonic beam source produces a variety of ions of the form $H^+(CO)_nAr_m$. We were able to select the protonated monomer ion HCO^+Ar and study it with photodissociation via elimination of argon, obtaining a spectrum consistent with those reported previously by other groups.[30,32] This spectrum is shown in Figure S1 of the Supplemental Information file. It has the expected C–H stretch at 2815 cm^{-1} and the carbonyl stretch at 2135 cm^{-1}. This spectrum also has additional bands not predicted by the scaled harmonic theory used in that figure.

We also observed efficient photodissociation of the $H^+(CO)_2Ar$ complex by the elimination of argon throughout the mid-IR. Figure 1 shows the experimentally measured IR-PD spectrum of $H^+(CO)_2Ar$ (upper trace) compared to that of the corresponding deuterated species $D^+(CO)_2Ar$ (lower trace). In the $H^+(CO)_2Ar$ spectrum, bands are observed at 1146, 1445, 2066, 2128, 2383, 2597, and 2772 cm^{-1}. For the deuterated ion a different pattern is observed, with bands at 1011, 1117, 1462, 1663, 1752, 2072, and 2480 cm^{-1}. Because of the conditions of the experiment and past experience with many similar systems, these ions are expected to be cold

(10–30K). All of the linewidths in these spectra are greater than the laser linewidth, as is commonly seen for photodissociation spectra, and attributed to predissociation lifetime effects. The additional widths for certain band features (e.g., the 2772 cm^{-1} band for $H^+(CO)_2$, or the 1462 and 2300–2400 cm^{-1} features for $D^+(CO)_2$) is believed to arise from the overlap of multiple unresolved bands in these regions. These widths are not likely to arise from any elevated temperature for these ions, as other bands in other parts of the same spectrum measured under the same conditions are much sharper. The unresolved features are likely to arise from combinations with low frequency stretching and bending modes of the tag atom (e.g., argon), which frequently occur in photodissociation spectra employing tagging. An additional possibility for bands involving O–H or O–D vibrations is the same kind of spectral diffusion dynamics that causes hydrogen bonding vibrations to be broadened in water-containing clusters.[47-50]

The bands in the $H^+(CO)_2Ar$ spectrum at 2066 and 2128 cm^{-1} can immediately be assigned to C–O stretch vibrations. The 2128 cm^{-1} band is only slightly lower in frequency than the 2135 cm^{-1} C–O stretch in the Ar-HCO^+ monomer ion. The observation of two bands here implies either that there are two kinds of CO molecules in the complex, or that there are two different isomers present. However, other features of these spectra are quite surprising. A strong band at 2772 cm^{-1} for $H^+(CO)_2Ar$ apparently shifts to lower energy (2480 cm^{-1}) upon deuteration. This has a frequency and isotopic shift consistent with a C–H stretch vibration. It is only slightly lower in frequency than the C–H stretch in the monomer HCO^+-Ar complex at 2815 cm^{-1}.[30,32] However, there should be no C–H stretch in the expected PBD structure. Indeed, the study of $H^+(CO)_2$ by Fortenberry *et al.* predicts the highest IR-active vibration for the PBD structure to be the antisymmetric C–O stretch at 2246 cm^{-1}.[84] The attachment of argon usually

occurs at an exposed proton site, if one is present, and causes a significant red shift in any vibration involving such a proton. If the 2772 cm^{-1} band is a C–H stretch, then the tag-free molecule would have a band at even higher frequency than the feature observed here. There is also no band near 1185 cm^{-1}, which was predicted as a weak feature for the perpendicular proton vibration of the PBD structure.[84] Therefore, these various band positions and isotopic shifts appear to be inconsistent with a linear proton-bound dimer.

It is important to note that the dissociation yield in spectra such as these may be affected by the binding energy of the tag atom, and thus low energy bands are sometimes not detected efficiently. In the present spectra, dissociation is detected for the $D^+(CO)_2Ar$ species in the region down to just below 1000 cm^{-1}. This places an upper limit on the argon binding energy to this complex. Therefore, assuming a comparable argon binding energy, low frequency bands in the $H^+(CO)_2Ar$ spectrum, such as the perpendicular proton stretch predicted at 1185 cm^{-1}, could have been detected here also if there were strong signal. The OPO laser tuning range ends at about 700 cm^{-1}, and therefore the strong parallel-proton stretch predicted by Terrill and Nesbitt[81] at 386 cm^{-1} or by Fortenberry *et al.*[84] at 316.5 cm^{-1} for the PBD structure cannot be accessed with the present experiment.

B. *p*-H_2 matrix isolation infrared absorption experiments

To further investigate this system, we conducted *p*-H_2 matrix isolation experiments. Such experiments have no mass selection, but they have a wider scanning range in the infrared. Because direct absorption is measured, their band intensities are not affected by photodissociation yields. Vibrational band shifts may occur in matrix isolation experiments comparable in magnitude, but not necessarily in the same direction, as those seen with tagging in gas phase experiments. To produce ions in this environment and to identify their spectra in the

presence of spectra from the more abundant neutrals requires a careful procedure which has been established in previous experiments.[104-106]

To produce $H^+(CO)_2$ ions in the hydrogen matrix, electron bombardment was carried out during the slow (8.5 h) deposition of a CO/*p*-H_2 (1/1000) mixture. Infrared spectroscopy of this matrix produced lines previously assigned to CO, CO_2, HCO, H_2CO, H_2O, and HO_2 as shown in trace (a) of Figure S2 in the Supplemental Information. Several lines not identified previously (marked as A^+ and B^+) also appeared as weak features in this spectrum. This matrix was maintained in darkness for 19 h, followed by irradiation at 254 nm; the difference spectra showing the results of these experimental steps are presented in traces (b) and (c) of Figure S2, respectively. In the difference spectra, lines pointing upward indicate generation and those pointing downward indicate decomposition. The intensity of a line at 2893.9 cm^{-1} marked as A^+ decreased significantly after 19 h in darkness, whereas those of lines in group B^+ at 1100.4, 1525.7, 2007.3, 2032.6, 2508–2528, and 2618–1682 cm^{-1} decreased slightly (trace b). These lines in group B^+ were mostly depleted upon irradiation at 254 nm (trace c). The decay after maintenance of the electron-bombarded matrix in darkness indicates that carriers of lines in groups A^+ and B^+ are cationic species because of their slow reactions with the trapped electrons.

To further distinguish the carriers, experiments were performed with varied mixing ratios of CO/*p*-H_2. Figure S3 shows partial infrared spectra of electron bombarded CO/*p*-H_2 mixtures with mixing ratios 1/700, 1/1000, and 1/2000; these spectra were normalized with respect to the intensity of the line A^+ at 2893.9 cm^{-1}. The intensities of lines in group B^+ increased with the mixing ratio of CO/*p*-H_2 relative to that of the line at 2893.9 cm^{-1} in group A^+, suggesting that lines in groups A^+ and B^+ most likely originate from HCO^+ and $H^+(CO)_2$ respectively. Consistent with this, a band at 2840 cm^{-1} was reported in the IR-PD study of HCO^+-H_2 by Bieske *et al.* and assigned to the C–H stretch of this ion.[29] As reported previously[30,32] and shown in

Figure S1, the corresponding C–H stretch of HCO^+-Ar occurs at 2815 cm^{-1}. All of these matrix or complexed values are significantly shifted to the red from the gas phase C–H stretch of formyl cation, which occurs at 3088.7 cm^{-1}.[21,22]

Similar experiments were performed with mixtures of CO/*n*-D_2. After deposition of a mixture of CO/*n*-D_2 (1/550) at 3.2 K with electron-bombardment for 6 h, many lines were observed (Figure S4(a)). Because the mobility of electrons in solid *n*-D_2 at 3.2 K is limited, the matrix was irradiated with an LED at 365 nm to release trapped electrons. A difference spectrum recorded upon irradiation of the matrix at 365 nm is shown in Figure S4(b); lines at 2514.7, 2032.2, 2005.3, 1809.1, 1651.5, 1347.4, and 1295.0 cm^{-1} were mostly depleted. Partial IR spectra recorded for electron bombarded CO/*n*-D_2 matrices with mixing ratios 1/550, 1/2000, and 1/10000 are compared in Figure S5. These spectra were normalized to the intensity of the line in group X^+ at 2514.7 cm^{-1}. The relative intensities of lines in group X^+ (at 2514.7, 1809.1, 1347.2, and 1295.4 cm^{-1}) were retained in these experiments, whereas relative intensities of lines in group Y^+ (at 2032.2, 2005.3, and 1651.5 cm^{-1}) increased with mixing ratios of CO. According to the comparison with theoretically predicted spectra and the IR-PD spectrum for $D^+(CO)_2Ar$, we assigned lines in X^+ to $D^+(CO)_2$ in solid *n*-D_2, and lines in group Y^+ to $D^+(CO)_3$. The absence of lines of DCO^+ is likely due to a low abundance and/or severe interferences from other species.

C. Comparison of IR-PD and *p*-H_2 experiments

Figure 2 shows a comparison of the gas phase IR-PD spectra for $H^+(CO)_2Ar$ and to the *p*-H_2 "difference" matrix spectra, where the bands corresponding to each other in the two spectra are connected with dashed red lines. The red asterisks indicate bands assigned to known species other than $H^+(CO)_2$, as indicated in Figure S2. Each band in the gas phase spectrum except the

one at 2383 cm^{-1} has a counterpart in the matrix spectrum. The bands in the matrix spectrum are all sharper, and relative band intensities in the matrix spectrum are different from those of the corresponding features in the gas phase spectrum. The additional widths of the bands in the gas phase spectra was discussed earlier. There are also significant shifts in band positions between the two spectra. Except for the matrix band at 1525.7 cm^{-1}, all other features are shifted to frequencies lower than those of the corresponding gas phase spectrum by 50–100 cm^{-1}. The shift is most noticeable for the intense gas phase band at 2772 cm^{-1}, which is tentatively associated with a C–H stretch. The corresponding multiplet feature in the matrix spectrum at 2618–2682 cm^{-1} is less intense compared to other bands. It should be noted that the gas phase spectrum has not been corrected for the laser power, which is highest at higher frequencies and gradually declines toward lower frequencies. Therefore, the intensity of the gas phase band at 2772 cm^{-1} may be enhanced by the greater laser power here and possibly by a greater dissociation yield at this higher photon energy. The most intense bands in the matrix spectrum are the two at 2007.3 and 2032.6 cm^{-1} in the region of the carbonyl stretches. The corresponding gas phase bands at 2066 and 2128 cm^{-1} have somewhat weaker relative intensities. The position of the bands in the gas phase spectrum may be shifted somewhat by the attachment of argon, but this should affect mostly the mode(s) associated with the argon attachment site. If the band at 2772 cm^{-1} is a free C–H stretch, argon would likely be attached at the exposed hydrogen, and this band would have a greater shift than the others whose vibrations are remote from the argon (i.e., the carbonyl stretches). The matrix environment apparently shifts all the bands. The differences between the gas phase and matrix spectra are therefore somewhat understandable. Similar differences between gas phase and *para*-hydrogen spectra, with missing bands, different band positions and intensities, etc., were also observed for the protonated dimer of CO_2.[58,73]

Figure 3 shows a comparison between the gas phase and matrix spectra for the deuterated $D^+(CO)_2$ species, obtained using the same methods. Here, the gas phase spectrum has several resolved features, but only two closely matching bands can be identified in the matrix spectrum. Again, the matrix bands are sharper, and the relative intensities in the two spectra do not match. A very weak feature in the matrix spectrum at 1347.2 cm^{-1} does not match anything in the gas phase spectrum, but is perhaps closest to the gas phase band at 1462 cm^{-1}. The relatively intense band at 2072 cm^{-1} in the gas phase spectrum does not appear in the matrix spectrum. Surprisingly, the two clear bands in the matrix spectrum are shifted to higher frequencies than the corresponding features in the gas phase spectrum, whereas most bands were red shifted in the $H^+(CO)_2$ spectrum. Different band shifts for H_2 vs D_2 matrices are not uncommon because of the softer versus more rigid environments.

Although the gas phase and matrix spectra have noticeable differences, they agree on several important issues. The general pattern of bands in the $H^+(CO)_2$ spectrum is reproduced in both measurements. They both detect bands at high frequency, consistent with a free C–H stretch, and bands near 2500 cm^{-1} for $D^+(CO)_2$ consistent with a C–D stretch. Both spectra have two distinct bands in the carbonyl stretching region for the $H^+(CO)_2$ spectrum. This pattern changes significantly for $D^+(CO)_2$ in the gas phase spectrum, whereas the matrix spectrum finds nothing here. Most importantly, neither experiment detects a band near 1185 cm^{-1} for $H^+(CO)_2$ where the perpendicular proton stretch has been predicted. The gas phase spectrum has a weak band at 1146 cm^{-1} and the matrix spectrum has one at 1100.4 cm^{-1}, which might correspond to this, but neither has particularly strong intensity. Neither experiment can access the lower frequency region where the parallel proton stretch band was predicted. Altogether, these results suggest that the main carrier of the infrared spectrum in both the gas phase and the *p*-H_2 matrix is

a structure other than the proton-bound dimer. We therefore have carried out computational work to locate other possible isomers that might explain these spectra.

D. Computational results

We conducted both density functional theory and ab initio calculations to predict structures and spectra for various isomers of $H^+(CO)_2$ that might be present in the experiments. Using successive geometry optimizations at the B3LYP/aug-cc-pVTZ and CCSD(T)/ANO1 levels of theory, we located a total of six isomers, which are shown in Figure 4. In addition to these structures, their relative energies are given (CCSD(T)/ANO1 level of theory, with zero-point correction). Figure 4 shows the energies of the tag-free clusters; the relative energies for both the tag-free and tagged structures are given in Table I. As shown in the Supplemental Information, the tagging with argon has only a minor effect on ion structures and their spectra, with the noted exception of somewhat greater shifts for the O–H (O–D) stretching vibrations where the argon is attached. Consistent with previous work, the lowest energy isomer **1** is the proton-bound dimer of CO, where the two carbon atoms are connected to the central proton. In isomer **2**, one of the CO units is rotated, such that the oxygen is pointing towards the proton. This structure is +5.1 (5.2 for D) kcal mol^{-1} higher in energy than isomer **1**. In isomers **3** and **4**, the structure is no longer linear, but bent by about 80 degrees. In both of these isomers, the angle of the CO with respect to the carbonyl of HCO^+ is close to 100°, which in organic chemistry is the "Bürgi-Dunitz approach angle" for nucleophilic attack at a carbonyl group.[109] Isomer **3** is +5.8 (5.9 for D) kcal mol^{-1} higher in energy than isomer **1**, whereas isomer **4** is +7.8 (8.0 for D) kcal mol^{-1} higher. The structures of these isomers differ only by the rotation of the hydrogen-bonded CO; in isomer **3** its carbon points towards the proton, while in isomer **4** its oxygen points toward the proton. Isomer **5** is a PBD of the form $CO\text{-}H^+\text{-}OC$; it has a relative energy of +30.1

(32.2 for D) kcal mol^{-1}. The last isomer (**6**) is a covalently bonded $OCCOH^+$ ion, which has a relative energy of +48.1 (50.9 for D) kcal mol^{-1}. Isomer **6** is shown with the *t,t* conformation, but it also has the *c,t* conformation according to B3LYP/aug-cc-pVTZ. However, the H_2 and Ar complexes of the latter seem to be unstable. Table I shows the relative energies and argon binding energies of all these $H/D^+(CO)_2$ isomers. The detailed structures and harmonic frequencies of all these computed isomers and their argon tagged species are provided in the Supplemental Information.

For comparison with the IR-PD spectra of $H^+(CO)_2Ar$ and $D^+(CO)_2Ar$, anharmonic vibrational spectra were calculated at the CCSD(T)/ANO1 level of theory; predicted anharmonic wavenumbers of isomers **1**–**4** are summarized in Tables II and III for $H^+(CO)_2Ar$ and $D^+(CO)_2Ar$, respectively, where they are compared to the experimental band positions. These isomers are deemed most relevant based on their spectra (see below). Tables II and III present only the most intense bands predicted by theory for these isomers. The full list of anharmonic band intensities for all the isomers is presented in the Supplemental Information as Table S1. According to our theory, the most stable isomer **1** of $H^+(CO)_2Ar$ has an intense band predicted at 1226 cm^{-1} (2381 km/mol), corresponding to the OC–H^+ stretch vibration, analogous to the parallel shared-proton stretch. However, this frequency may be an artifact of our computations, which optimized to the linear but non-centrosymmetric $OCH^+(CO)$ structure found previously by other groups.[79,81] Both Terrill and Nesbitt[81] and Fortenberry *et al.*[84] suggested that the actual structure of the proton-bound dimer is dynamically averaged to be centrosymmetric, and then the shared-proton stretching vibration would occur at a much lower frequency (386 or 315.6 cm^{-1}, respectively). The only high frequency vibrations predicted by Fortenberry for the centrosymmetric structure are a relatively weak perpendicular proton stretch (1184.9 cm^{-1}) and a moderate intensity carbonyl stretch (2246.3 cm^{-1}), higher than anything in the experiment in this

region. Our isomer **1** has weak bands in the carbonyl stretching region, but these are also at frequencies higher than those in the experiment. The deuterated isotopologue is predicted by our theory to have a parallel proton-stretch band at 980 cm^{-1}, which is subject to the same possible artifact. Neither our non-centrosymmetric isomer **1** nor Fortenberry's dynamically averaged centrosymmetric structure has the main vibrational features detected experimentally, and therefore we examine the spectra of other isomers.

Isomers **2**–**4** all have higher frequency bands and carbonyl stretches with significant intensities. The argon tagged isomer **2** has an $O–CH^+$ carbonyl stretch band predicted at 2118 cm^{-1}, an OCH^+(C–O) stretch at 2049 cm^{-1}, and an $OC–H^+$ stretch at 2752 cm^{-1}. For the deuterated isotopologue, bands are predicted at 1735 (symmetric $O–C–D^+$ stretch), 2054 (OCD^+(C–O) stretch), and 2464 ($OC–D^+$ stretch) cm^{-1}. The argon tagged isomer **3** has a strong $O–CH^+$ carbonyl stretch band predicted at 2128 cm^{-1}, an OCH^+(C–O) stretch at 2175 cm^{-1}, and an $OC–H^+$ stretch at 2896 cm^{-1}. For the deuterated isotopologue, bands are predicted at 1810 (symmetric $O–C–D^+$ stretch), 2175 (OCD^+(C–O) stretch), and 2504 (antisymmetric $O–C–D^+$ stretch) cm^{-1}. For the proton version of argon tagged isomer **4**, anharmonic theory predicts bands at 2068, 2128, and 2859 cm^{-1}. These frequencies are associated with the OCH^+(O–C) stretch (2068 cm^{-1}), the $O–CH^+$ stretch (2128 cm^{-1}), and the $OC–H^+$ stretch (2859 cm^{-1}) vibrations, respectively. The deuterated isomer **4** is predicted to have corresponding bands at 1791 (symmetric $O–C–D^+$ stretch), 2068 (OCD^+(O–C) stretch), and 2499 (antisymmetric $O–C–D^+$ stretch) cm^{-1}. Interestingly, the predicted $O–CH^+$ carbonyl stretch band has the same frequency (2128 cm^{-1}) for both isomers **3** and **4**, and the respective "external" C–O (2175 cm^{-1}) or O–C (2068 cm^{-1}) stretches are the same for the H or D isotopologues of these isomers.

E. Comparison of experiments with calculations

Figure 5 shows the experimental IR-PD spectrum compared to the spectra predicted by our anharmonic theory for argon-tagged isomers **1**–**4** of $H^+(CO)_2$. Other isomers have spectra with less agreement with the experiment than these (see Supplemental Information, Figure S6). As shown, isomers **3** and **4** have structures with a CH group attached to argon, producing "free" C–H stretches at high frequency. The frequencies predicted (2896 and 2859 cm^{-1}) are higher than the band detected at 2772 cm^{-1}, but the intensities of these vibrations match the IR-PD experiment reasonably well for both of these isomers. As noted earlier, the proton-bound isomer **1** has no strong band at high frequency. Isomer **2** has a linear OCH^+–OC structure, with the interaction weak enough to produce a high frequency OC–H^+ stretch at 2752 cm^{-1}. This band is also intense, but falls at a lower frequency than the experimental band at 2772 cm^{-1}. The spectra for isomers **2** and **4** both have moderate intensity bands for two carbonyl stretches, whereas isomer **1** has only a very weak band here and isomer **3** has only one strong band. The bands for isomer **4** at 2068 and 2128 cm^{-1} match almost perfectly with those in the experiment at 2066 and 2128 cm^{-1} and they have nearly the same intensity ratio as that in the experiment. Weak OC–H^+ bend overtones are predicted for isomers **2**, **3** and **4** near 1600–1700 cm^{-1}, but there is nothing in the experiment corresponding to these. There is also nothing in the theory for any of these isomers explaining the weak/broad bands in the experiment at 2383 and 2597 cm^{-1}. On the basis of these comparisons, it seems that the spectrum predicted for isomer **4** matches the experiment better than any other, although the agreement is not perfect.

To understand the interactions of H_2 (or D_2) with $H^+(CO)_2$ (or $D^+(CO)_2$), we performed computations on the $H^+(CO)_2H_2$ and $D^+(CO)_2D_2$ complexes with the B3LYP/aug-cc-pVTZ method. The isomers identified for these complexes are similar to those found for $H^+(CO)_2Ar$,

with an H_2 molecule replacing argon. Structures of isomers **3** and **4** are shown in Figure S9. In Figure S10 we compared the experimental spectrum of $H^+(CO)_2$ in solid *p*-H_2 with predicted anharmonic vibrational wavenumbers of isomers **3** and **4** of $H^+(CO)_2H_2$ (Table S3). Similar to $H^+(CO)_2Ar$, the observed lines at 2618–2682, 2032.6, 2007.3 cm^{-1} agree best with those predicted for isomer **4** at 2786, 2173, and 2117 cm^{-1} (Table II); the observed wavenumber of the C–H^+ stretching mode near 2650 cm^{-1} is red-shifted from calculations, likely because the proton was shared with more than one H_2. The line observed at 1525.7 cm^{-1} might correspond to the overtone predicted at 1623 cm^{-1} for isomer **4**, whereas the line observed at 1100.4 cm^{-1} has no corresponding predicted line except a weak overtone line predicted at 915 cm^{-1} for isomer **4**

Figure 6 shows a comparison of the gas phase spectrum for the deuterated ion with that predicted by anharmonic theory. Again, isomer **1** has no strong bands predicted at high frequency, but both isomers **3** and **4** have medium-intensity features predicted (2504 and 2499 cm^{-1}, respectively) that match the experimental band at 2480 cm^{-1} reasonably well. Isomer **2** has a weaker band at the slightly lower frequency of 2464 cm^{-1}. Isomers **2**, **3** and **4** each have two C–O stretches that are much more widely separated than they were for the $H^+(CO)_2$ species. The pair at 1735 and 2054 cm^{-1} for isomer **2** and that at 1791 and 2068 cm^{-1} for isomer **4** match the experiment better than that at 1809 and 2175 cm^{-1} for isomer **3**. Again, isomer **4** matches the band positions and relative intensities in the experiment better than the other isomers, and the agreement for the three highest frequency bands is quite good. Isomer **2** also provides a reasonable match to the experiment. However, none of the isomers account for the experimental structure below 1700 cm^{-1}, where several broad bands are detected. The bands near 1011, 1117 and 1663 cm^{-1} could conceivably be accounted for by a minor population of isomer **1**, but nothing accounts for the stronger broad feature at 1462 cm^{-1}. The isolated sharp bands in the

experiment at 1752 and 2072 cm^{-1} seem to indicate the presence of only one isomer with these bands rather than contributions from multiple isomers.

In Figure S11 we compared the experimental spectrum of $D^+(CO)_2$ in solid D_2 with anharmonic vibrational wavenumbers of $D^+(CO)_2D_2$ isomers predicted with the B3LYP/aug-cc-pVTZ method (Table S4). Similar to $D^+(CO)_2Ar$, the observed lines at 2514.7 and 1808.9 cm^{-1} agree the best with lines predicted for isomer **4** at 2520 and 1752 cm^{-1}; an intense line predicted at 2116 cm^{-1} was unidentified because of the severe interference from absorption of CO and its complexes. Two weak lines observed at 1347.2 and 1295.4 cm^{-1} might correspond to the overtone lines predicted at 1451 and 1357 cm^{-1} for isomer **4**.

From these spectra for the $H^+(CO)_2Ar$ and $D^+(CO)_2Ar$ ions, it can be seen that a single isomer (**4**) can account for the majority of the resolved spectral features for both isotopologues. Isomer **2** is perhaps the next closest match, but it has some vibrational features (intensity pattern in the carbonyl stretching region for $H^+(CO)_2Ar$ and weak high frequency band for $D^+(CO)_2Ar$) where the agreement is less satisfactory. Additionally, the lack of more complex multiplet patterns in the region of the C–H, C–D and C–O stretching regions implies that there is either only one isomer present or that other minor isomers have no strong bands in these regions. This means that isomers **3** or **6** are not likely to be present, but small amounts of isomers **1** could conceivably be present, explaining some of the weaker signals in these spectra. The most stable isomer **1** should have a perpendicular proton stretch in the 1100 (H) or 900 (D) cm^{-1} regions, but no strong bands are detected here, suggesting that this isomer is not present in high concentration. Therefore, the additional structure in these spectra, in the 2300–2600 cm^{-1} (H) or 1000–1500 cm^{-1} (D) regions, likely comes from additional overtone or combination bands of isomer **4** whose positions or intensities are not captured by the present level of anharmonic

theory. For example, the deuterated species has in-plane and out-of-plane DCO^+ bending modes at 682 and 706 cm^{-1}. A combination of these vibrations, perhaps together with the argon stretch at 116 cm^{-1}, might explain the structure near 1462 cm^{-1}. Combinations of these bends with the carbonyl stretch at 1752 cm^{-1} might explain the structure in the 2300–2400 cm^{-1} region. The VPT2 method employed here can only predict intensities for transitions from the vibrational ground state to excited states with up to two quanta in energy. Transitions to higher energy states are assigned zero intensity regardless of experimentally observable IR activity.

In solid *p*-H_2 and *n*-D_2, we also found that the high-energy isomer **4** was produced. Producing a higher-energy conformer has been reported by Wong et al. in the UV-irradiated β-alanine in solid *p*-H_2,[110] but they also detected predominantly the lowest energy isomer. The predominant formation of only isomer **4** in solid *p*-H_2 might be explained by a mechanism in which the protonation of CO or $(CO)_2$ is followed by rapid complexation or solvation with *p*-H_2. The initial protonation of a CO molecule by H_3^+ leads to the formation of $OCH^+\cdots H_2$, which prevents the second CO to form isomer **1** ($OC\cdots H^+\cdots CO$). Another possible mechanism is the direct protonation of $(CO)_2$ which somehow leads to the formation of isomer **4**. This latter mechanism was investigated computationally, and the details are presented in the Supplementary Material. Because of the small difference in proton affinities of CO (594 kJ mol^{-1}) and H_2 (422 kJ mol^{-1}), once the protonation of CO by H_3^+ occurs, the H_2 product prefers to partially share the transferred proton and maintain a nearly linear $OCH^+\cdots H_2$ structure (considering H_2 has a spherical wave function). The second CO can hence partially share the proton perpendicularly; isomers **3** and **4** both have a nearly linear substructure of OCH^+-H_2. As discussed in the Supplemental Information, protonation of low-energy structures of $(CO)_2$ produces only isomer **4**, consistent with our experimental observation. However, formation of isomer **3** from

protonation of high-energy $(CO)_2$ cannot be completely excluded because these "high-energy" structures are only higher in energy by less than 0.17 kcal mol^{-1} from theory.

F. Additional IR-PD experiments

On the basis of our spectroscopy experiments and their comparison to theory, it seems that isomer **4**, which is computed to be less stable by 7.8 kcal/mol than the most stable isomer **1**, is the most abundant species produced in both the molecular beam and hydrogen matrix experiments. Although the agreement with theory for this isomer is not definitive, it seems to be clear that the most stable isomer **1** is produced either not at all, or in low enough concentrations to make it difficult to detect. We therefore have considered a number of possible kinetic effects that might explain the preferential formation of the less stable isomer. One possibility is a concentration bias that might limit the access of CO to its most stable binding site. The IR-PD experiments were carried out with a large excess of argon buffer gas. If the more abundant argon binds to the proton of HCO^+ on average before a CO molecule does, it could conceivably block the preferred in-line binding site for CO. The binding energy of argon in the Ar-HCO^+ complex has been computed previously by Botschwina (D_0 = 4.37 kcal/mol),[35] and it is substantial, especially at the low temperature of the experiment. A second CO molecule arriving after argon has attached might not be able to displace it, and would then bind in the next best position coming in from the side. A similar issue might affect the hydrogen matrix data, where H_2 is present in large excess compared to CO and can also bind efficiently at the proton of HCO^+ (D_0 = 2.43 kcal/mol).[29] To address these possibilities, we decided to use neon tagging to measure the spectrum. Neon is predicted to have a much smaller binding energy to HCO^+ (0.9 kcal/mol at CCSD(T)/ANO1), making it less likely to block the binding of CO. Additional experiments used an expansion of CO/H_2/He in a 10:30:260 pressure ratio and measured the spectrum of $H^+(CO)_3$.

Presumably, if the tagging atom is eliminated, CO should be able to find its preferred binding site and the extra CO would be weakly bound, acting as the tag species to enable photodissociation. Additional computational work was done on $H^+(CO)_2Ne$ and $H^+(CO)_3$ at the same level of theory described earlier.

Figure 7 shows the IR-PD spectrum of $H^+(CO)_2Ne$, compared to the spectra predicted by several low-lying isomers of this ion. This spectrum is more complex than that measured with argon tagging, with a multiplet of at least five bands at high frequency (2874, 2968, 3012, 3043, and 3066 cm^{-1}), and two (2171 and 2308 cm^{-1}) in the general region of the C–O stretch. Surprisingly, the bands at high frequency are much sharper than those seen with argon tagging. However, different linewidths from different tag atoms are not uncommon in ion spectroscopy measured with photodissociation because of different predissociation dynamics. The anharmonic vibrational spectra predicted for the several isomers of this ion are presented in the lower traces of the Figure. As shown, no spectrum for any single isomer matches the experimental spectrum. Only isomers **2**, **3**, **4** and **6** have any bands at high frequency, and each of these isomers has just one band each predicted here. The bands in the 2874–3066 cm^{-1} region are all at frequencies higher than the C–H stretch of $H^+(CO)_2Ar$, consistent with a smaller red-shift for similar vibrations when tagging with neon as opposed to argon. It is tempting on the basis of the multiplet here to suggest that more than one isomer is present, but the C–O stretch region is quite simple, with only two clear bands. This suggests that there might be only one isomer present, but that the high frequency region has complex anharmonic structure not captured by this level of theory. The VPT2 method used here cannot reproduce multiple quanta (>2) combinations or Fermi-resonances, which may occur in this region. Low frequency stretches of the neon atom or the CO group near 100 and 200 cm^{-1} could produce combination bands with a C–H stretch, explaining some of the additional structure here. The prediction of

two C–O stretches is consistent with the spectra predicted for isomers **2** and **4**, but the frequencies of these isomers don't match the experiment well at all. In particular, the 2308 cm^{-1} frequency seems to be quite high for a C–O stretch. Considering all of this, it is not possible to conclude what the structure of the neon-tagged species is. However, there are no strong bands in the 1100–1400 cm^{-1} region, where the proton-bound dimer structure should have its perpendicular proton stretch, and there is much structure at high frequency where free C–H stretches are expected for more than one structure. It seems that there is still no solid evidence for a PBD structure, but rather additional data supporting one or more asymmetric structures.

Figure 8 shows the spectrum measured for the $H^+(CO)_3$ ion in an expansion of CO seeded with hydrogen compared to the spectra predicted by theory for this ion. Because there is no rare gas in the expansion mixture, and therefore no tagging atom, this experiment eliminates any possible effects of competitive binding at the OCH^+ charge site. The spectrum consists of broad structure near 1683 cm^{-1}, a weak band at 2065 cm^{-1}, a strong, sharp band at 2186 cm^{-1}, and additional broad structure at high frequency centered near 2721 cm^{-1}. The broad structure near 1683 cm^{-1} was not seen for the other tagged ions, the 2065 and 2186 cm^{-1} bands are in the region seen before for carbonyl stretches, and the band at 2721 cm^{-1} is quite close to the high frequency band seen for $H^+(CO)_2Ar$. The most stable structure identified by theory (isomer **7**) is a non-centrosymmetric proton-bound dimer with a third CO molecule bound weakly to the side of the linear PBD axis, carbon-in, analogous to the argon-tagged isomer **1**. Isomer **8** has the same structure, but with the external CO rotated to have oxygen-in. Isomer **9** has a similar non-centrosymmetric structure, but both CO groups interacting with the OCH^+ ion are oxygen-in. Isomer **10** is a 32.7 kcal/mol less stable centrosymmetric structure, with all three CO molecules having oxygen-in orientations.

The comparison of the spectra predicted for these isomers to that in the experiment shows that no single isomer is able to account for the major bands measured. Isomers **7** and **8** both have strong bands at low frequency from the HC–O^+ stretch of an isolated HCO^+ ion in a non-centrosymmetric structure. The band for isomer **7** is much closer to the broad 1683 cm^{-1} band in the experiment. Isomer **7** also has a weak C–H stretch of the HCO^+ moiety predicted at 2324 cm^{-1}, where there is a weak signal in the experiment. However, neither isomer **7** or **8** has a carbonyl stretch with any significant intensity near 2186 cm^{-1}, and neither of these has a C–H stretch at higher frequency that could explain the broad 2721 cm^{-1} band. Isomer **9** has this kind of band, but no bands predicted near 1683 cm^{-1}. Therefore, at least two isomers of $H^+(CO)_3$ must be present to explain the spectrum. A combination of isomers **7** and **9** could explain bands in the general vicinity of those measured, but there is no detailed match between experiment and theory. Multiple isomers or combinations with low-frequency bends and stretches of the excess CO may explain the additional widths of the bands in this spectrum.

It should be noted that isomer **7** here is analogous to isomer **1** for $H^+(CO)_2Ar$, with a linear OCH^+-CO configuration that is non-centrosymmetric. We mentioned earlier that previous theory had obtained such a structure initially for $H^+(CO)_2$, which was dynamically averaged to a centrosymmetric PBD configuration. If the barrier to proton transfer is similar here, the same kind of dynamical averaging could take place for $H^+(CO)_3$. To investigate this possibility, we have used single-point energy calculations for the centrosymmetric complexes of $H^+(CO)_2$, $H^+(CO)_2Ar$ and $H^+(CO)_3$ (see Supplemental Information). The argon and CO complexes were each confirmed to be transition states with the argon or CO located orthogonal to the OC-H^+-CO axis in a "T"-shaped C_{2v} structure. We find the energies of these transition states to be 1.20, 1.32 and 2.03 kcal/mol relative to the respective non-centrosymmetric equilibrium structures. Our value for $H^+(CO)_2$ is virtually the same as that found in previous work.[81,84] The values for the

argon and CO complexes show that complexation tends to raise the barrier slightly, making the non-centrosymmetric structure slightly more favored. However, the zero-point energy in each of these complexes is still slightly above the barrier height, suggesting that a delocalized centrosymmetric structure should form. The computational results therefore suggest that a centrosymmetric proton-bound dimer structure should form regardless of the tagging situation. Unfortunately, the experiments do not agree with this assertion, particularly for the $H^+(CO)_3$ complex. It has a high frequency band that can only be explained by a free C–H^+ stretch, and the 1683 cm^{-1} feature comes from the C–O stretch of an isolated HCO^+ unit. These patterns are inconsistent with a centrosymmetric structure.

The extensive spectroscopy measurements and theory reported here therefore leave us with a conundrum about the structure of the $H^+(CO)_2$ ion. All computational studies are in agreement that the proton-bound dimer structure (isomer **1** here) lies lowest in energy, and that the zero-point energy should cause the non-centrosymmetric structure to become centrosymmetric. Unfortunately, there is no evidence for this in the spectroscopy. We have obtained several spectra for this ion tagged with argon, neon or an extra CO, as well as in a hydrogen matrix isolation environment. The detailed assignments of these spectra are less than perfect, but this can largely be attributed to the shortcomings of the VPT2 anharmonic theory computations. Zero-point effects apparently cause the computations of frequencies at the electronic minima to be inadequate for many of these complexes. However, all the spectra agree that the species measured have high frequency C–H stretches, only one or two C–O stretches, and no bands where shared-proton vibrations would be expected. Figure 9 shows the comparison of the IR-PD spectra for $H^+(CO)_2Ar$, $H^+(CO)_2Ne$ and $H^+(CO)_3$, which demonstrates their similarity. Although kinetic effects of how the ions are produced may influence some of these systems, the $H^+(CO)_3$ complex is particularly problematic, as any such issues should be

eliminated for this ion. Nonetheless, it exhibits a strong C–H stretch, only one C–O stretch, and a reasonably strong low-frequency feature assigned to the C–O stretch of an "isolated" HCO^+ moiety. It is clear from these spectra that a large population of ions produced under a variety of conditions form non-centrosymmetric structures. But the question remains: Are any ions forming the predicted centrosymmetric proton-bound dimer structure?

Unfortunately, it is quite difficult to be sure about the possibility of a centrosymmetric PBD structure co-existing with the other isomers indicated by our spectra. According to the available theory on this system, its only intense infrared feature would be the parallel proton stretch vibration located at a frequency below 400 cm^{-1},[81] which is outside the range of any of the experiments. A band for the perpendicular proton stretch is predicted near 1185 cm^{-1}, but with weak intensity (11 km/mol).[84] It is therefore not too surprising that we detect nothing here. The only other band with significant intensity is the carbonyl stretch predicted at 2246 cm^{-1} (intensity 53 km/mol).[84] This is in the range of our experiment and could have been detected. The carbonyl stretching bands are sharp for the most part and there are only one or two bands here in each spectrum, consistent with patterns expected for the other most abundant isomers as we assigned them. If there were a significant amount of the centrosymmetric PBD isomer, we should have seen additional carbonyl stretches for at least some of the spectra, but we do not. It is conceivable that an additional carbonyl stretch from the PBD ion is present, but overlapped by other bands or weaker than predicted. For this reason, and the other issues mentioned here, we cannot rule out the presence of the centrosymmetric PBD structure. However, as shown here, a substantial population, if not the majority, of these ions adopt other structures. This behavior has not been seen for any other proton-bound dimer ions to our knowledge.

Additional experiments beyond the scope of our present work could be done in the future to further explore the structure of this ion. High resolution absorption spectroscopy, like that

already done for HCO^+ could of course be done for the $H^+(CO)_2$ ion without any tagging or trapping environment. A high frequency C–H stretch, or the carbonyl stretch, would be in the range of available laser systems. Likewise, it would be especially interesting to explore the spectrum at low frequencies (<400 cm^{-1}) where the shared proton stretch is predicted for the PBD structure. This could be done in the gas phase using a free electron laser, or perhaps in a hydrogen matrix using far-infrared light sources and detectors. Additional computational studies could re-examine the effects of dynamical averaging on the spectroscopy, perhaps including the effects of argon or neon tagging. Such computations are beyond the scope of the present study, and indeed would be quite challenging. The proton-bound dimer of CO remains as a fundamentally important structural problem, with significant implications for astrochemistry.

IV. Conclusion

We report the first infrared spectroscopy for the $H^+(CO)_2$ and $D^+(CO)_2$ molecular ions, complemented by extensive computational chemistry. In gas phase experiments, this ion is studied via tagging with argon, neon, or an additional CO using infrared photodissociation spectroscopy. Additional experiments employ *p*-H_2 matrix isolation absorption spectroscopy. The gas phase spectrum for $H^+(CO)_2Ar$ matches that measured for $H^+(CO)_2$ in *p*-H_2. Both have patterns that can be assigned to non-linear structures different from the linear centrosymmetric proton-bound dimer structure predicted to be most stable. Additional spectra measured with neon tagging or with an excess CO ligand also have features consistent with a free C–H stretch that are inconsistent with a PBD structure. Computational studies using anharmonic vibrational theory identify several low energy isomers other than the centrosymmetric PBD structures that account for the measured spectral patterns. A substantial population of isomers other than the

most stable PBD structure are definitely present, but it is not clear whether or not the PBD structure is in fact formed.

Supplemental Information

See Supplemental Information for optimized geometries and harmonic frequencies of all computed isomers. Also shown are the anharmonic spectra predicted for the remaining argon-tagged, neon-tagged, and CO trimer isomers not presented in the main article. The details of computational results on the formation of $H^+(CO)_2H_2$ isomers are presented.

Data Availability Statement

The data that supports the findings of this study are available within the article [and its Supplemental Information].

Acknowledgements

This work was supported by the National Science Foundation (grant No. CHE-1764111), Ministry of Science and Technology, Taiwan (grant No. MOST108-2639-M009-001-ASP and MOST108-3017-F009-004) and the Center for Emergent Functional Matter Science of National Chiao Tung University from The Featured Areas Research Center Program within the framework of the Higher Education Sprout Project by the Ministry of Education (MOE) in Taiwan. Japan Society for the Promotion of Science (JSPS KAKENHI grant No. JP18K03717) partially supported this work. The National Center for High-Performance Computation in Taiwan and the High Performance Computing Center in Hokkaido University provided computer time. D.L. and J.P.W. are thankful to the Alexander von Humboldt Foundation for postdoctoral fellowships.

References

1. E. Herbst, W. Klemperer, "The formation and depletion of molecules in dense interstellar clouds," Astrophys. J. **185**, 505 (1973).
2. D. Smith, "The ion chemistry of interstellar clouds," Chem. Rev. **92**, 1473 (1992).
3. T. W. Hartquist, D. A. Williams, *The Molecular Astrophysics of Stars and Galaxies*, Clarendon Press, Oxford, 1998.
4. A. G. G. M. Tielens, *The Physics and Chemistry of the Interstellar Medium*, Cambridge University Press, 2005.
5. S. Petrie, D. K. Böhme, "Ions in space," Mass Spectrom. Rev. **26**, 258 (2007).
6. T. P. Snow, V. M. Bierbaum, "Ion chemistry in the interstellar medium," Annu. Rev. Anal. Chem. **1**, 229 (2008).
7. W. Klemperer, "Astronomical chemistry," Annu. Rev. Phys. Chem. **62**, 173 (2011).
8. W. D. Geppert, M. Larsson, "Experimental investigations into astrophysically relevant ionic reactions," Chem. Rev. **113**, 8872 (2013).
9. M. Mladenović, E. Roueff, "Ion-molecule reactions involving HCO^+ and N_2H^+: Isotopologue equilibria from new theoretical calculations and consequences for interstellar isotope fractionation," Astron. Astrophys. **566**, A144 (2014).
10. E. Herbst, "The synthesis of large interstellar molecules," Int. Rev. Phys. Chem. **36**, 287 (2017).
11. W. Klemperer, V. Vaida, "Molecular complexes in close and far away," Proc. Nat. Acad. Sci. **103**, 10584 (2006).
12. W. Klemperer, "Interstellar chemistry," Proc. Nat. Acad. Sci. **103**, 12232 (2006).
13. D. Buhl, L. E. Snyder, "Unidentified interstellar microwave line," Nature **228**, 267

(1970).

14. W. Klemperer, "Carrier of the interstellar 89.190 GHz line," Nature **227**, 1230 (1970).

15. E. Herbst, W. Klemperer, "Is X-ogen HCO^+?" Astrophys. J. **188**, 255 (1974).

16. R. C. Woods, T. A. Dixon, R. J. Saykally, P. G. Szanto, "Laboratory microwave spectrum of HCO^+," Phys. Rev. Lett. **35**, 1269 (1975).

17. K. V. L. N. Sastry, E. Herbst, F. C. De Lucia, "Millimeter and submillimeter spectra of HCO^+ and DCO^+," J. Chem. Phys. **75**, 4169 (1981).

18. R. C. Woods, R. J. Saykally, T. G. Anderson, T. A. Dixon, P. G. Szanto, "The molecular structure of HCO^+ by the microwave substitution method," J. Chem. Phys. **75**, 4256 (1981).

19. F. Tinti, L. Bizzocchi, C. Degli Esposti, L. Dore, "Improved rest frequencies of HCO^+ at 1 THz," Astrophys. J. **669**, L113 (2007).

20. G. Cazzoli, L. Cludi, G. Buffa, C. Puzzarini, "Precise THz measurements of HCO^+, N_2H^+, and CF^+ for astrophysical observations," Astrophys. J. Suppl. Ser. **203**, 11 (2012).

21. C. S. Gudeman, M. H. Begemann, J. Pfaff, R. J. Saykally, "Velocity modulated infrared laser spectroscopy of molecular ions: The ν_1 band of HCO^+," Phys. Rev. Lett. **50**, 727 (1983).

22. T. Amano, "The ν_1 fundamental band of HCO^+ by difference frequency laser spectroscopy," J. Chem. Phys. **79**, 3595 (1983).

23. S. C. Foster, A. R. W. McKellar, T. J. Sears, "Observation of the ν_3 fundamental band of HCO^+," J. Chem. Phys. **81**, 578 (1984).

24. P. B. Davies, P. A. Hamilton, W. J. Rothwell, "Infrared laser spectroscopy of the ν_3 fundamental of HCO^+," J. Chem. Phys. **81**, 1598 (1984).

25. P. B. Davies, W. J. Rothwell, "Diode laser detection of the bending mode of HCO^+," J.

Chem. Phys. **81**, 5239 (1984).

26. K. Kawaguchi, C. Yamada, S. Saito, E. Hirota, "Magnetic field modulated infrared laser spectroscopy of molecular ions: The ν_2 band of HCO^+," J. Chem. Phys. **82**, 1750 (1985).

27. T. Nakanaga, T. Amano, "Infrared detection of HOC^+ by difference frequency laser spectroscopy," J. Mol. Spec. **121**, 502 (1987).

28. M. Mladenović, "Theoretical spectroscopic parameters for isotopic variants of HCO^+ and HOC^+," J. Chem. Phys. **147**, 114111 (2017).

29. E. J. Bieske, S. A. Nizkorodov, F. R. Bennett, J. P. Maier, "The infrared spectrum of the H_2-HCO^+ complex," J. Chem. Phys. **102**, 5152 (1995).

30. S. A. Nizkorodov, O. Dopfer, T. Ruchti, M. Meuwly, J. P. Maier, E. J. Bieske, "Size effects in cluster infrared spectra: The ν_1 band of Ar_n-HCO^+ (n = 1–13)," J. Phys. Chem. **99**, 17118 (1995).

31. H. Linnartz, T. Speck, J. P. Maier, "High-resolution infrared spectrum of the ν_3 band in Ar-HCO^+," Chem. Phys. Lett. **288**, 504 (1998).

32. S. A. Nizkorodov, O. Dopfer, M. Meuwly, J. P. Maier, E. J. Bieske, "Mid-infrared spectra of the proton-bound complexes Ne_n-HCO^+ (n = 1,2)," J. Chem. Phys. **105**, 1770 (1996).

33. T. Salomon, M. Töpfer, P. Schreier, S. Schlemmer, H. Kohguchi, L. Surin, O. Asvany, "Double resonance rotational spectroscopy of He-HCO^+," Phys. Chem. Chem. Phys. **21**, 3440 (2019).

34. K. O. Sullivan, G. I. Gellene, "Ab initio study of Ar_n-HCO^+ (n = 0–6): Insight into size dependent cluster ion properties," Int. J. Mass. Spectrom. **201**, 121 (2000).

35. P. Botschwina, R. Oswald, "Coupled cluster calculations for Ar–HCO^+," J. Molec. Struc. **599**, 371 (2001).

36. R. P. Bell, *The Proton in Chemistry*, Cornell University Press, Ithaca, NY, 1959.

37. E. Caldin and V. Gold, eds., *Proton Transfer Reactions*, Chapman and Hall, London, 1975.

38. J. T. Hynes, J. P. Klinman, H.-H. Limbach, R. L. Schowen, eds., *Hydrogen Transfer Reactions*, Vols. 1–4, Wiley-VCH Publishers, Weinheim, 2006.

39. A. G. Harrison, *Chemical Ionization Mass Spectrometry*, Second Edition, CRC Press, Boca Raton, FL, 1992.

40. S. A. McLuckey, D. Cameron, R. G. Cooks, "Proton affinities from dissociations of proton-bound dimers," J. Am. Chem. Soc. **103**, 1313 (1981).

41. J. W. Larson, T. B. McMahon, "Formation, thermochemistry, and relative stabilities of proton-bound dimers of oxygen n-donor bases from ion cyclotron resonance solvent-exchange equilibria measurements," J. Am. Chem. Soc. **104**, 6255 (1982).

42. W. Y. Feng, M. Goldenberg, C. Lifshitz, "Reactions of proton-bound dimers," J. Amer. Soc. Mass Spectrom. **5**, 695 (1994).

43. R. G. Ewing, G. A. Eicemen, J. A. Stone, "Proton-bound cluster ions in ion mobility spectrometry," Int. J. Mass Spectrom. **193**, 57 (1999).

44. M. Meot-Ner, "The ionic hydrogen bond," Chem. Rev. **105**, 213 (2005).

45. R. S. Blake, P. S. Monks, A. M. Ellis, "Proton-transfer reaction mass spectrometry," Chem. Rev. **109**, 861 (2009).

46. K. R. Asmis, N. L. Pivonka, G. Santambrogio, M. Brümmer, C. Kaposta, D. M. Neumark, L. Wöste, "Gas-phase infrared spectrum of the protonated water dimer," Science **299**, 1375 (2003).

47. J. M. Headrick, E. G. Diken, R. S. Walters, N. I. Hammer, R. A. Christie, J. Cui, E. M. Myshakin, M. A. Duncan, M. A. Johnson, K. D. Jordan, "Spectral signatures of hydrated

proton vibrations in water clusters," Science **308**, 1765 (2005**)**.

48. J. M. Headrick, J. C. Bopp, M. A. Johnson, "Predissociation spectroscopy of the argon-solvated $H_5O_2^+$ "Zundel" cation in the 1000–1900 cm^{-1} region," J. Chem. Phys. **121**, 11523 (2004).

49. E. G. Diken, J. M. Headrick, J. R. Roscioli, J. C. Bopp, M. A. Johnson, A. B. McCoy, "Fundamental excitations of the shared proton in the $H_3O_2^-$ and $H_5O_2^+$ complexes," J. Phys. Chem. A **109**, 1487 (2005).

50. N. I. Hammer, E. G. Diken, J. R. Roscioli, M. A. Johnson, E. M. Myshakin, K. D. Jordon, A. B. McCoy, X. Huang, J. M. Bowman, S. Carter, "The vibrational predissociation spectra of the $H_5O_2^+RG_n$ (RG=Ar, Ne) clusters: Correlation of the solvent perturbations in the free OH shared proton transitions of the Zundel ion," J. Chem. Phys. **122**, 244301 (2005).

51. T. D. Fridgen, L. MacAleese, P. Maître, T. B. McMahon, P. Boissel, J. Lemaire, "Infrared spectra of homogeneous and heterogeneous proton-bound dimers in the gas phase," Phys. Chem. Chem. Phys. **7**, 2747 (2005).

52. T. D. Fridgen, L. MacAleese, T. B. McMahon, J. Lemaire, P. Maître, "Gas phase infrared multiple-photon dissociation spectra of methanol, ethanol and propanol proton-bound dimers, protonated propanol and the propanol/water proton-bound dimer," Phys. Chem. Chem. Phys. **8**, 955 (2006).

53. J. R. Roscioli, L. R. McCunn, M. A. Johnson, "Quantum structure of the intermolecular proton bond," Science **316**, 249 (2007).

54. T. Pankewitz, A. Lagutschenkov, G. Niedner-Schatteburg, S. S. Xantheas, Y.-T. Lee, "Infrared spectrum of $NH_4^+(H_2O)$: Evidence for mode specific fragmentation," J. Chem. Phys. **126**, 074307 (2007).

55. Y. Yang, O. Kühn, G. Santambrogio, D. J. Goebbert, K. R. Asmis, "Vibrational signatures of hydrogen bonding in the protonated ammonia clusters $NH_4^+(NH_3)_{1-4}$" J. Chem. Phys. **129**, 224302 (2008).

56. G. H. Gardenier, J. R. Roscioli, M. A. Johnson, "Intermolecular proton binding in the presence of a large electric dipole: Ar-tagged vibrational predissociation spectroscopy of the $CH_3CN{\cdot}H^+{\cdot}OH_2$ and $CH_3CN{\cdot}D^+{\cdot}OD_2$ complexes," J. Phys. Chem. A **112**, 12022 (2008).

57. G. E. Douberly, A. M. Ricks, B. W. Ticknor, M. A. Duncan, "The structure of protonated acetone and its dimer: Infrared photodissociation spectroscopy from 800–4000 cm^{-1}," Phys. Chem. Chem. Phys. **10**, 77 (2008).

58. G. E. Douberly, A. M. Ricks, B. W. Ticknor, M. A. Duncan, "The structure of protonated carbon dioxide clusters: Infrared photodissociation spectroscopy and ab initio calculations," J. Phys. Chem. A **112**, 950 (2008).

59. G. E. Douberly, A. M. Ricks, B. W. Ticknor, W. C. McKee, P. v. R. Schleyer, M. A. Duncan, "Infrared photodissociation spectroscopy of protonated acetylene and its clusters," J. Phys. Chem. A **112**, 1897 (2008).

60. A. M. Ricks, G. E. Douberly, M. A. Duncan, "Infrared spectroscopy of the protonated nitrogen dimer: The complexity of shared proton vibrations," J. Chem. Phys. **131**, 104312 (2009).

61. T. C. Cheng, B. Bandyopadhyay, Y. Wang, B. J. Braams, J. M. Bowman, M. A. Duncan, "The shared proton mode lights up the infrared spectrum of fluxional cations H_5^+ and D_5^+," J. Phys. Chem. Lett. **1**, 758 (2010).

62. G. E. Douberly, R. S. Walters, J. Cai, K. D. Jordan, M. A. Duncan, "Infrared spectroscopy of small protonated water clusters $H^+(H_2O)_n$ (n = 2–5): Isomers, argon

tagging and deuteration," J. Phys. Chem. A **114**, 4570 (2010).

63. B. Bandyopadhyay, T. C. Cheng, M. A. Duncan, "Proton sharing in hydronium-nitrogen clusters probed with infrared spectroscopy," Int. J. Mass Spectrom. **297**, 124 (2010).

64. T. C. Cheng, L. Jiang, K. R. Asmis, Y. Wang, J. M. Bowman, A. M. Ricks, M. A. Duncan, "Mid- and far-IR spectra of H_5^+ and D_5^+ compared to the predictions of anharmonic theory," J. Phys. Chem. Lett. **3**, 3160 (2012).

65. T. C. Cheng, B. Bandyopadhyay, J. D. Mosley, M. A. Duncan, "Protonation in water-benzene nanoclusters: Hydronium, Zundel and Eigen at a hydrophobic interface," J. Am. Chem. Soc. **134**, 13046 (2012).

66. D. C. McDonald, D. T. Mauney, D. Leicht, J. H. Marks, J. A. Tan, J. -L. Kuo, M. A. Duncan, "Trapping a proton in argon: Spectroscopy and theory of the proton-bound argon dimer and its solvation," J. Chem. Phys. **145**, 231101 (2016).

67. J. P. Wagner, D. C. McDonald II, M. A. Duncan, "Infrared spectroscopy of the astrophysically relevant protonated formaldehyde dimer," J. Phys. Chem. A **122**, 192 (2018).

68. J. P. Wagner, D. C. McDonald II, M. A. Duncan, "Spectroscopy of proton coordination with ethylenediamine," J. Phys. Chem. A **122**, 5168 (2018).

69. D. C. McDonald II, J. P. Wagner, A. B. McCoy, M. A. Duncan, "Near-infrared spectroscopy of protonated water clusters: Higher elevations in the hydrogen bonding landscape," J. Phys. Chem. Lett. **9**, 5664 (2018).

70. P. R. Franke, M. A. Duncan, G. E. Douberly, "Infrared photodissociation spectroscopy and anharmonic vibrational study of the HO_4^+ molecular ion," J. Chem. Phys., in press.

71. M. Boyer, D. C. McDonald II, J. P. Wagner, J. E. Colley, D. S. Orr, M. A. Duncan, A. B. McCoy, "The role of tunneling in the spectra of H_5^+ and D_5^+ up to 7300 cm^{-1}," J. Phys.

Chem. A **124**, 4427 (2020).

72. M. Tsuge, J. Kalinowski, R. B. Gerber, Y.-P. Lee, "Infrared identification of proton-bound rare-gas dimers $(XeHXe)^+$, $(KrHKr)^+$, and $(KrHXe)^+$ and their deuterated species in solid hydrogen," J. Phys. Chem. A. **119**, 2651 (2015).

73. P. Das, M. Tsuge, Y.-P. Lee, "Infrared absorption of *t*-$HOCO^+$, $H^+(CO_2)_2$, and HCO_2^- produced in electron bombardment of CO_2 in solid *para*-H_2," J Chem. Phys. **145**, 014306 (2016).

74. H.-Y. Liao, M. Tsuge, J. A. Tan, J.-L. Kuo, Y.-P. Lee, "Infrared spectra and anharmonic coupling of proton-bound nitrogen dimers N_2-H^+-N_2, N_2-D^+-N_2, and $^{15}N_2$-H^+-$^{15}N_2$ in solid *para*-hydrogen," Phys. Chem. Chem. Phys. **19**, 20484 (2017).

75. K. R. Jennings, J. V. Headley, R. S. Mason, "The temperature dependence of ion-molecule association reactions," Int. J. Mass Spectrom. Ion Phys. **45**, 315 (1982).

76. M. Mladenović, E. Roueff, "Ion-molecule reactions involving HCO^+ and N_2H^+: Isotopologue equilibria from new theoretical calculations and consequences for interstellar isotope fractionation," Astron. Astrophys. **566**, A144 (2014).

77. D. Verdes, H. Linnartz, J. P. Maier, P. Botschwina, R. Oswald, P. Rosmus, P.J. Knowles, "Spectroscopic and theoretical characterization of linear centrosymmetric $NN{\cdot\cdot}H^+{\cdot\cdot}NN$," J. Chem. Phys. **111**, 8400 (1999).

78. P. Botschwina, T. Dutoi, M. Mladenovic, R. Oswald, S. Schmatz, H. Stoll, "Theoretical investigations of proton-bound cluster ions," Faraday Discuss. **118**, 433 (2001).

79. J. J. Szymczak, S. Roszak, R. W. Gora, J. Leszczynski, "Molecular properties of protonated homogeneous and mixed carbon oxide and carbon dioxide clusters," J. Chem. Phys. **119**, 6560 (2003).

80. B. Chan, J. E. Del Bene, L. Radom, "Proton-bound homodimers: How are the binding

energies related to proton affinities?," J. Am. Chem. Soc. **129**, 12197 (2007).

81. K. Terrill, D. J. Nesbitt, "*Ab initio* anharmonic vibrational frequency predictions for linear proton-bound complexes OC-H^+-CO and N_2-H^+-N_2," Phys. Chem. Chem. Phys. **12**, 8311 (2010).

82. C. E. Cotton, J. S. Francisco, R. Linguerri, A. O. Mitrushchenkov, "Structural and spectroscopic study of the van der Waals complex of CO with HCO^+ and the isoelectronic complex of CS with HCS^+," J. Chem. Phys. **136**, 184307 (2012).

83. Q. Yi, J. M. Bowman, R. C. Fortenberry, J. S. Mancini, T. J. Lee, T. D. Crawford, W. Klemperer, J. S. Francisco, "Structure, anharmonic vibrational frequencies, and intensities of $NNHNN^+$," J. Phys. Chem. A **119**, 11623 (2015).

84. R. C. Fortenberry, Q. Yu, J. S. Mancini, J. M. Bowman, T. J. Lee, T. D. Crawford, W. F. Klemperer, J. S. Francisco, "Spectroscopic consequences of proton delocalization in $OCHCO^+$," J. Chem. Phys. **143**, 071102 (2015).

85. M. A. Duncan, "Infrared laser spectroscopy of mass-selected carbocations," J. Phys. Chem. A **116**, 11477 (2012).

86. D. S. Cornett, M. Peschke, K. LaiHing, P. Y. Cheng, K. F. Willey, M. A. Duncan, "A reflectron time-of-flight mass spectrometer for laser photodissociation," Rev. Sci. Instrum. **63**, 2177 (1992).

87. M. Okumura, L. I. Yeh, J. D. Myers, Y. T. Lee, "Infrared spectra of the cluster ions $H_7O_3^+ \cdot H_2$ and $H_9O_4^+ \cdot H_2$," J. Chem. Phys. **85**, 2328 (1986).

88. M. Okumura, L. I. Yeh, Y. T. Lee, "Infrared spectroscopy of the cluster ions hydrogen triatomic monopositive ion-(molecular hydrogen)$_n$ ($H_3^+ \cdot (H_2)_n$)," J Chem. Phys. **88**, 79 (1988).

89. E. J. Bieske, J. P. Maier, "Spectroscopic studies of ionic complexes and clusters," Chem. Rev. **93**, 2603 (1993).

90. T. Ebata, A. Fujii, N. Mikami, "Vibrational spectroscopy of small-sized hydrogen-bonded clusters and their ions," Int. Rev. Phys. Chem. **17**, 331 (1998).

91. E. J. Bieske, O. Dopfer, "High resolution spectroscopy of cluster ions," Chem. Rev. **100**, 3963 (2000).

92. M. A. Duncan, "Frontiers in the spectroscopy of mass-selected molecular ions," Int. J. Mass Spectrom. **200**, 545 (2000).

93. M. A. Duncan, "Infrared spectroscopy to probe structure and dynamics in metal ion-molecule complexes," Int. Rev. Phys. Chem. **22**, 407 (2003).

94. N. R. Walker, R. S. Walters, M. A. Duncan, "Frontiers in the infrared spectroscopy of gas phase metal ion complexes," New J. Chem. **29**, 1495 (2005).

95. W. H. Robertson, M. A. Johnson, "Molecular aspects of halide ion hydration: The cluster approach," Annu. Rev. Phys. Chem. **54**, 173 (2003).

96. T. R. Rizzo, J. A. Stearns, O. V. Boyarkin, "Spectroscopic studies of cold, gas-phase biomolecular ions," Int. Rev. Phys. Chem. **28**, 481 (2009).

97. T. Baer, R. C. Dunbar, "Ion spectroscopy: Where did it come from; Where is it now; and where is it going?" J. Am. Soc. Mass Spectrom. **21**, 681 (2010).

98. M. Z. Kamrath, E. Garand, P. A. Jordan, C. M. Leavitt, A. B. Wolk, M. J. van Stipdonk, S. J. Miller, M. A. Johnson, "Vibrational characterization of simple peptides using cryogenic infrared photodissociation of H_2-tagged, mass-selected ions. J. Am. Chem. Soc. **133**, 6440 (2011).

99. J. G. Redwine, Z. A. Davis, N. L. Burke, R. A. Oglesbee, S. A. McLuckey, T. S. Zwier, "A novel ion trap based tandem mass spectrometer for the spectroscopic study of cold gas phase polyatomic ions," Int. J. Mass Spectrom. **348**, 9 (2013).

100. S. Chakrabarty, M. Holtz, E. K. Campbell, A. Banerjee, D. Gerlich, J. P. Maier, "A novel method to measure electronic spectra of cold molecular ions," J. Phys. Chem. Lett. **4**, 4051 (2013).

101. A. B. Wolk, C. M. Leavitt, E. Garand, M. A. Johnson, "Cryogenic ion chemistry and spectroscopy," Acc. Chem. Res. **47**, 202 (2014).

102. N. Heine, K. R. Asmis, "Cryogenic ion trap vibrational spectroscopy of hydrogen-bonded clusters relevant to atmospheric chemistry," Int. Rev. Phys. Chem. **34**, 1 (2015).

103. J. Roithová, A. Gray, E. Andris, J. Jašík, D. Gerlich, "Helium tagging infrared photodissociation spectroscopy of reactive ions," Acc. Chem. Res. **49**, 223 (2016).

104. M. Bahou, Y.-J. Wu, Y.-P. Lee, "A new method for investigating infrared spectra of protonated benzene ($C_6H_7^+$) and cyclohexadienyl radical (c-C_6H_7) using *p*-hydrogen," J. Chem. Phys. **136**, 154304 (2012).

105. M. Bahou, P. Das, Y.-F. Lee, Y.-J. Wu, Y.-P. Lee, "Infrared spectra of free radicals and protonated species produced in *para*-hydrogen matrices," Phys. Chem. Chem. Phys. **16**, 2200 (2014).

106. M. Tsuge, C.-Y. Tseng, Y.-P. Lee, "Spectroscopy of prospective interstellar ions and radicals isolated in *para*-hydrogen matrices," Phys. Chem. Chem. Phys. **20**, 5344 (2018).

107. M. J. Frisch, G. W. Trucks, H. B. Schlegel, G. E. Scuseria, M. A. Robb, J. R. Cheeseman, G. Scalmani, V. Barone, G. A. Petersson, H. Nakatsuji, X. Li, M. Caricato, A. V. Marenich, J. Bloino, B. G. Janesko, R. Gomperts, B. Mennucci, H. P. Hratchian, J. V. Ortiz, A. F. Izmaylov, J. L. Sonnenberg, D. Williams-Young, F. Ding, F. Lipparini, F.

Egidi, J. Goings, B. Peng, A. Petrone, T. Henderson, D. Ranasinghe, V. G. Zakrzewski, J. Gao, N. Rega, G. Zheng, W. Liang, M. Hada, M. Ehara, K. Toyota, R. Fukuda, J. Hasegawa, M. Ishida, T. Nakajima, Y. Honda, O. Kitao, H. Nakai, T. Vreven, K. Throssell, J. A. Montgomery Jr., J. E. Peralta, F. Ogliaro, M. J. Bearpark, J. J. Heyd, E. N. Brothers, K. N. Kudin, V. N. Staroverov, T. A. Keith, R. Kobayashi, J. Normand, K. Raghavachari, A. P. Rendell, J. C. Burant, S. S. Iyengar, J. Tomasi, M. Cossi, J. M. Millam, M. Klene, C. Adamo, R. Cammi, J. W. Ochterski, R. L. Martin, K. Morokuma, O. Farkas, J. B. Foresman, D. J. Fox, Gaussian09, Revision D. 01. (Gaussian, Inc., Wallingford, CT, 2016).

108. CFOUR, a quantum chemical program package written by J. F. Stanton, J. Gauss, M. E. Harding, P. G. Szalay, with contributions from A. A. Auer, R. J. Bartlett, U. Benedikt, C. Berger, D. E. Bernholdt, Y. J. Bomble, L. Cheng, O. Christiansen, M. Heckert, O. Heun, C. Huber, T.-C. Jagau, D. Jonsson, J. Jusélius, K. Klein, W. J. Lauderdale, D. A. Matthews, T. Metzroth, L. A. Mück, D. P. O'Neill, D. R. Price, E. Prochnow, C. Puzzarini, K. Ruud, F. Schiffmann, W. Schwalbach, S. Stopkowicz, A. Tajti, J. Vázquez, F. Wang, J. D. Watts; with the integral packages MOLECULE (by J. Almlöf and P. R. Taylor), PROPS (by P. R. Taylor), ABACUS (by T. Helgaker, H. J. Aa. Jensen, P. Jørgensen, and J. Olsen), and ECP routines by A. V. Mitin and C. van Wüllen, 2010.

109. H. B. Bürgi, J. D. Dunitz, J. M. Lehn, G. Wipff, "Stereochemistry of reaction paths at carbonyl centers," Tetrahedron **30**, 1563 (1974).

110. Y. T. Angel Wong, S. Y. Toh, P. Djuricanin, T. Momose, "Conformational composition and population analysis of β-alanine isolated in solid parahydrogen" J. Mol. Spectrosc. **310**, 23 (2015).

Table I. Relative energies and argon/neon binding energies computed at the CCSD(T)/ANO1 level of theory for the predicted isomers of $H^+(CO)_2$, $D^+(CO)_2$ and $H^+(CO)_3$.

Isomer	Relative Energy (kcal/mol)			Binding Energy (cm^{-1})	
	$H^+(CO)_2$	$H^+(CO)_2Ar$	$H^+(CO)_2Ne$	Ar	Ne
1	0.0	0.0	0.0	768	157
2	5.1	5.0	5.1	806	182
3	5.8	4.3	5.4	1315	293
4	7.8	6.1	7.4	1344	301
5	30.1	30.8	32.2	548	123
6	48.1	46.0	50.9	1517	358
	Relative Energy (kcal/mol)			Binding Energy (cm^{-1})	
	$D^+(CO)_2$	$D^+(CO)_2Ar$	$D^+(CO)_2Ne$	Ar	Ne
1	0.0	0.0	0.0	778	156
2	5.2	4.8	4.8	816	184
3	5.9	4.0	5.1	1310	297
4	8.0	5.9	7.1	1339	306
5	32.2	30.7	30.2	549	122
6	50.9	45.4	46.9	1493	360
	Relative Energy (kcal/mol)			Binding Energy (cm^{-1})	
	$H^+(CO)_3$			CO	
7	0.0			1455	
8	1.49			935	
9	6.22			982	
10	32.7			1050	

Table II. Band positions (in cm^{-1}) for $H^+(CO)_2$ in the IR-PD and matrix isolation experiments compared with VPT2 predictions for argon-tagged isomers **1**, **2**, **3**, and **4** at the CCSD(T)/ANO1 level of theory. Band intensities (km/mol) are given in parentheses.

Experiments		Theory				
IR-PD	*p*-H_2	Isomer **1**	Isomer **2**	Isomer **3**	Isomer **4**	Approx. Description[a]
2772	2618-2682 (100)[b]		2752 (912)	2896 (598)	2859 (661)	ν(OC-H^+)
				2872 (459)[b]	2786 (459)[b]	
2597	2508-2528 (20)					
2128	2032.6 (22)	2264 (42)	2118 (293)	2128 (328)	2128 (373)	ν(O-CH^+)
				2177 (366)[c]	2173 (325)[c]	
2066	2007.3 (36)	2163 (26)	2049 (409)	2175 (21)	2068 (142)	ν(CO)
				2254 (26)[c]	2117 (200)[c]	
				1933 (50)[c]	1788 (80)[c]	$2\omega_{oop}$(O-C-H^+)
	1525.7 (34)			1627 (36)[c]	1623 (60)[c]	$2\omega_{ip}$(O-C-H^+)
1445		1395 (72)				ν_s(OC-H^+) + ν_s(CH^+C)
1146	1100.4 (16)	1226 (2381)[d]				ν_s(OC-H^+)

[a] Mode description: ν: stretch; ω: bend; s: symmetric; oop: out-of-plane; ip: in-plane.

[b] Percentage integrated intensities relative to the most intense band near 2650 cm^{-1}.

[c] Anharmonic frequencies and IR intensities (km/mol) of $H^+(CO)_2H_2$ predicted at the B3LYP/aug-cc-pVTZ level of theory.

[d] This result might be a computational artifact: see text.

Table III. Band positions (in cm^{-1}) for $D^+(CO)_2$ in the IR-PD and matrix isolation experiments compared with VPT2 predictions for argon-tagged isomers **1**, **2**, **3**, and **4** at the CCSD(T)/ANO1 level of theory. Band intensities (km/mol) are given in parentheses.

Experiments		Theory				
IR-PD	*p*-H_2	Isomer **1**	Isomer **2**	Isomer **3**	Isomer **4**	Approx. Description[a]
2480	2514.7 (22)[b]		2464 (105)	2504 (88)	2499 (87)	ν(OC-D^+)
				2500 (89)[c]	2520 (36)[c]	
2072		2294 (17)	2054 (177)	2175 (21)	2068 (144)	ν(CO)
				2256 (28)[c]	2116 (198)[c]	
1752	1808.9 (100)	2211 (2)	1735 (599)	1810 (355)	1791 (427)	ν_s(O-C-D^+)
				1803 (338)[c]	1752 (390)[c]	
1663		1656 (49)				$2\omega_{oop}$(O-C-D^+)
1462	1347.2 (4)			1395 (14)	1394 (0.2)	$2\omega_{ip}$(O-C-D^+)
				1458 (19)[c]	1451 (33)[c]	
	1295.4 (11)			1299 (11)	1350 (0.5)	$2\omega_{ip}$(O-C-D^+)
				1260 (12)[c]	1357 (24)[c]	
1117		1168 (261)				ν_s(OCD^+) + ν_s(CD^+C)
1101		980 (664)				D^+ shuttling

[a] Mode description: ν: stretch; ω: bend; s: symmetric; oop: out-of-plane; ip: in-plane.

[b] Percentage integrated intensities relative to the most intense band near 1809 cm^{-1}.

[c] Anharmonic frequencies and IR intensities (km/mol) of $D^+(CO)_2D_2$ predicted at the B3LYP/aug-cc-pVTZ level of theory.

Figure Captions

Figure 1. Experimental infrared photodissociation (IR-PD) spectra of $H^+(CO)_2Ar$ (top) and $D^+(CO)_2Ar$ (bottom).

Figure 2. Comparison of the gas phase IR-PD spectrum of $H^+(CO)_2Ar$ (top) to the difference spectrum generated for the $H^+(CO)_2$ ion in *p*-H_2 (bottom). Infrared lines marked with asterisks are assigned to species other than $H^+(CO)_2$; see Figure S2.

Figure 3. Comparison of the gas phase IR-PD spectrum of $D^+(CO)_2Ar$ (top) to the difference spectrum generated for the $D^+(CO)_2$ ion in *n*-D_2 (bottom). Infrared lines marked with asterisks are assigned to species other than $D^+(CO)_2$; see Figure S4.

Figure 4. Geometries and ZPVE-corrected relative energies of six stable isomers of $H^+(CO)_2$ (and $D^+(CO)_2$) in kcal mol^{-1} as calculated at the CCSD(T)/ANO1 level of theory.

Figure 5. Comparison of the experimental infrared spectrum of $H^+(CO)_2Ar$ (top) with computed VPT2 spectra for isomers **1**–**4** (four lower traces, respectively) at the CCSD(T)/ANO1 level of theory.

Figure 6. Comparison of the experimental infrared spectrum of $D^+(CO)_2Ar$ (top) with computed VPT2 spectra for isomers **1**–**4** (four lower traces, respectively) at the CCSD(T)/ANO1 level of theory.

Figure 7. Experimental IR-PD spectra of $H^+(CO)_2Ne$ (top) compared to the predictions of theory for isomers **2**–**6** (four lower traces, respectively).

Figure 8. Experimental IR-PD spectrum of $H^+(CO)_3$ (top) compared to the spectra predicted by theory for isomers **7**–**10** (four lower traces, respectively) of this ion.

Figure 9. Comparison of the experimental IR-PD spectra for $H^+(CO)_3$ (top), $H^+(CO)_2Ar$ (middle), and $H^+(CO)_2Ne$ (bottom).

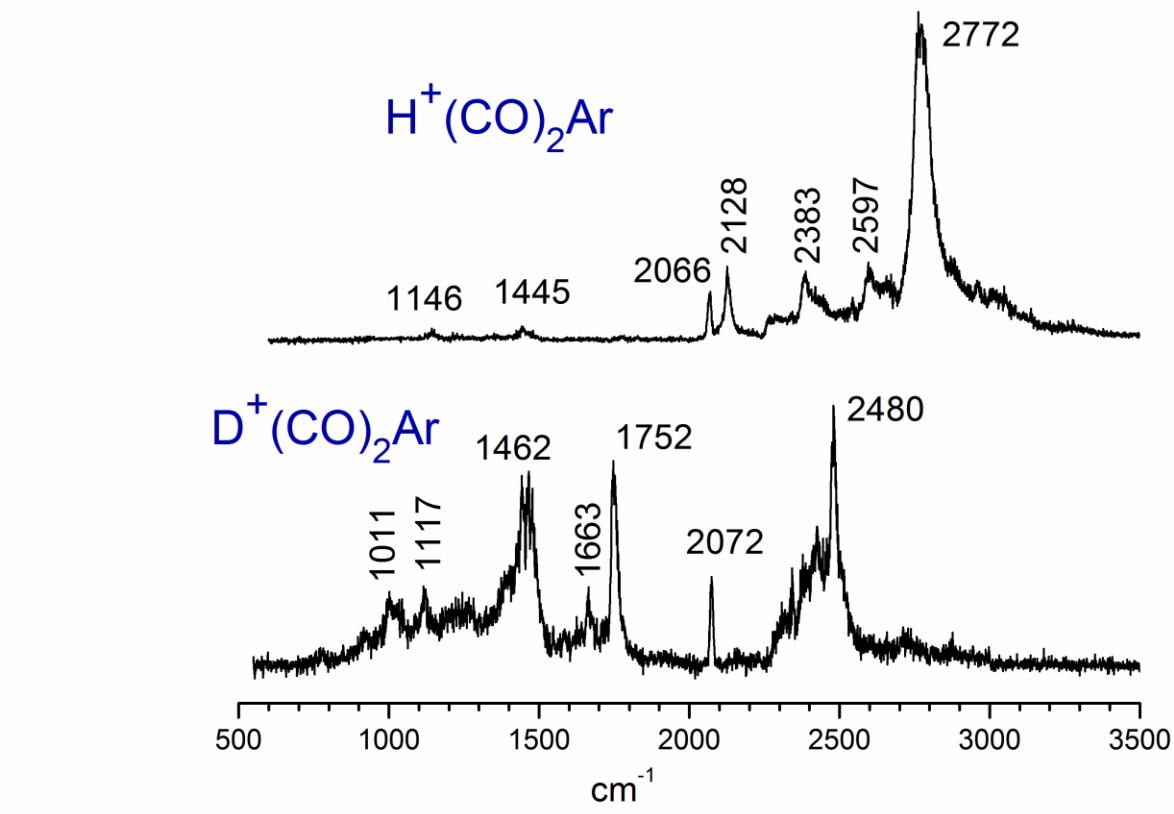
H+(CO)2Ar
2772
2597
2383
2128
2066
1445
1146
D+(CO)2Ar
2480
1752
1462
2072
1663
1117
1011
500
1000
1500
2000
2500
3000
3500
cm-1

Figure 1.

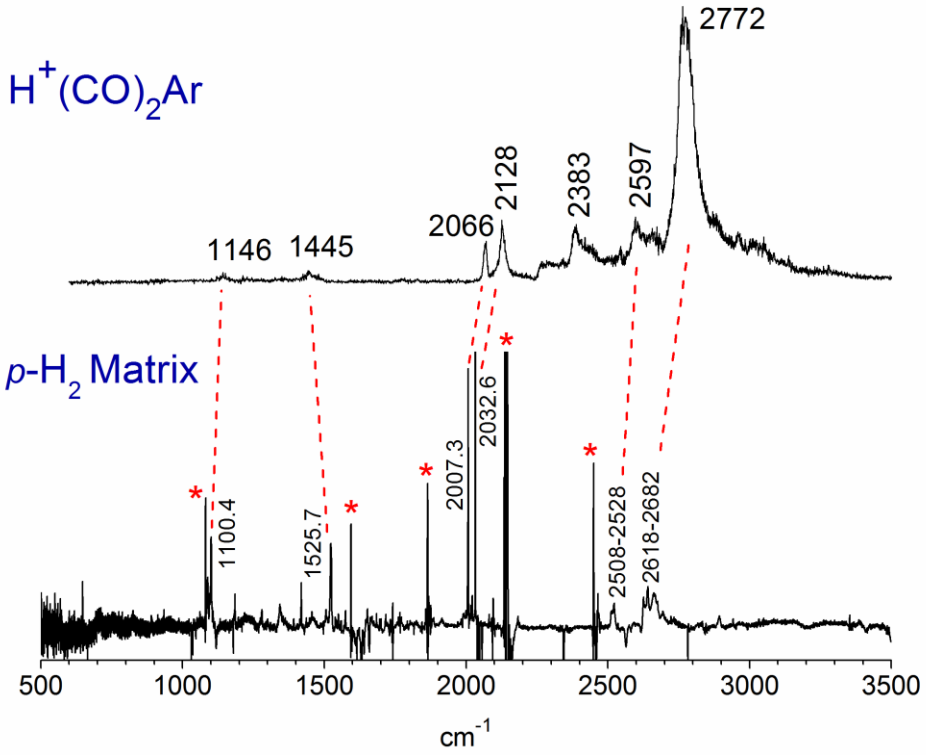
H+(CO)2Ar
2772
2597
2383
2128
2066
1146
1445
p-H2 Matrix
2032.6
2007.3
1525.7
1100.4
2508-2528
2618-2682
*
500
1000
1500
2000
2500
3000
3500
cm-1

Figure 2.

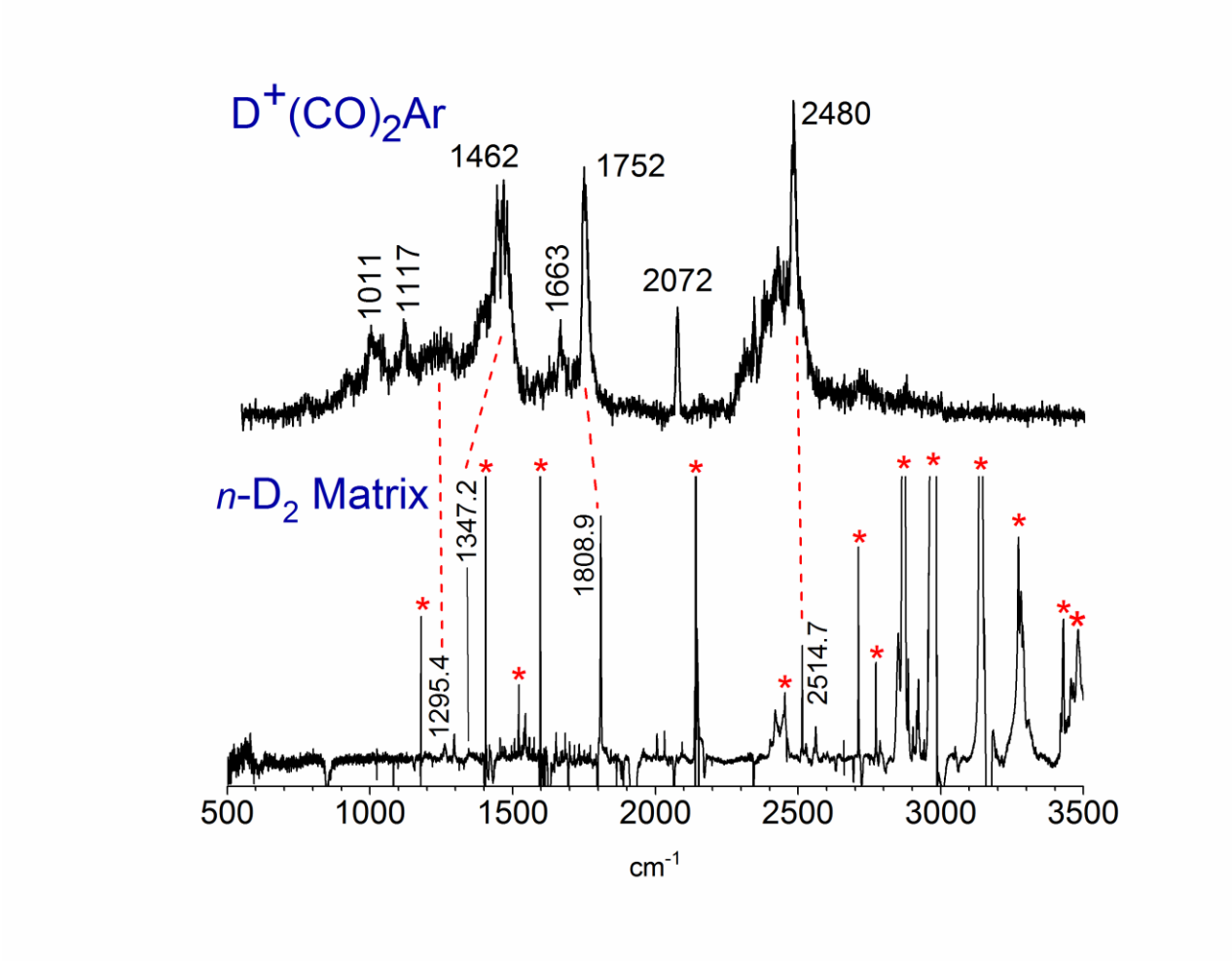
D+(CO)2Ar
2480
1462
1752
1011
1117
1663
2072
n-D2 Matrix
1347.2
1808.9
1295.4
2514.7
500
1000
1500
2000
2500
3000
3500
cm-1

Figure 3.

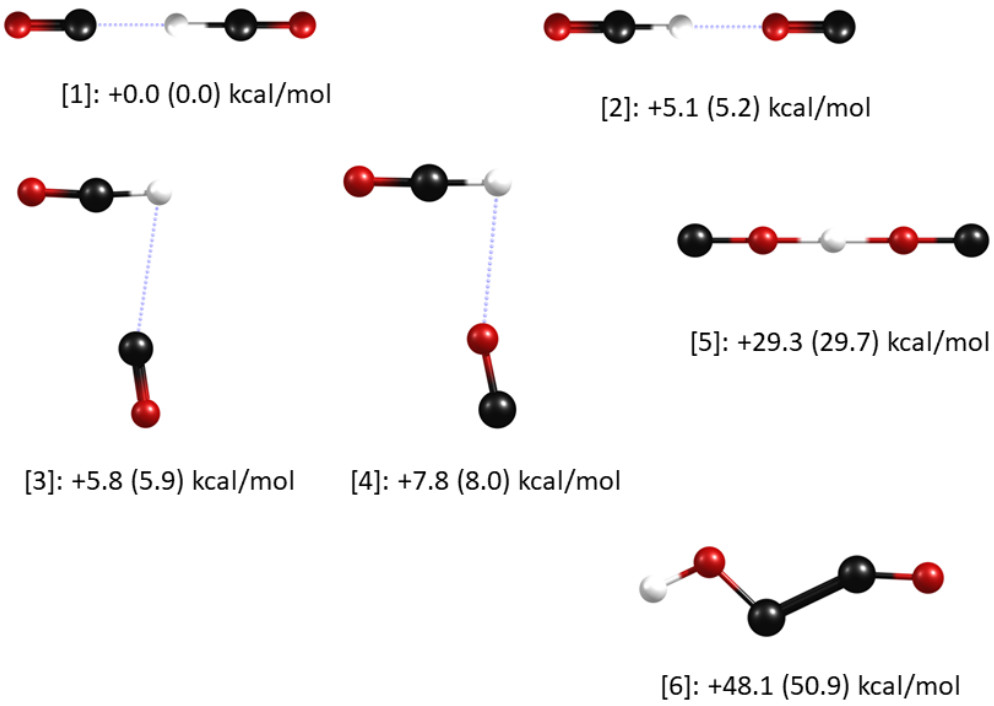
[1]: +0.0 (0.0) kcal/mol
[2]: +5.1 (5.2) kcal/mol
[3]: +5.8 (5.9) kcal/mol
[4]: +7.8 (8.0) kcal/mol
[5]: +29.3 (29.7) kcal/mol
[6]: +48.1 (50.9) kcal/mol

Figure 4.

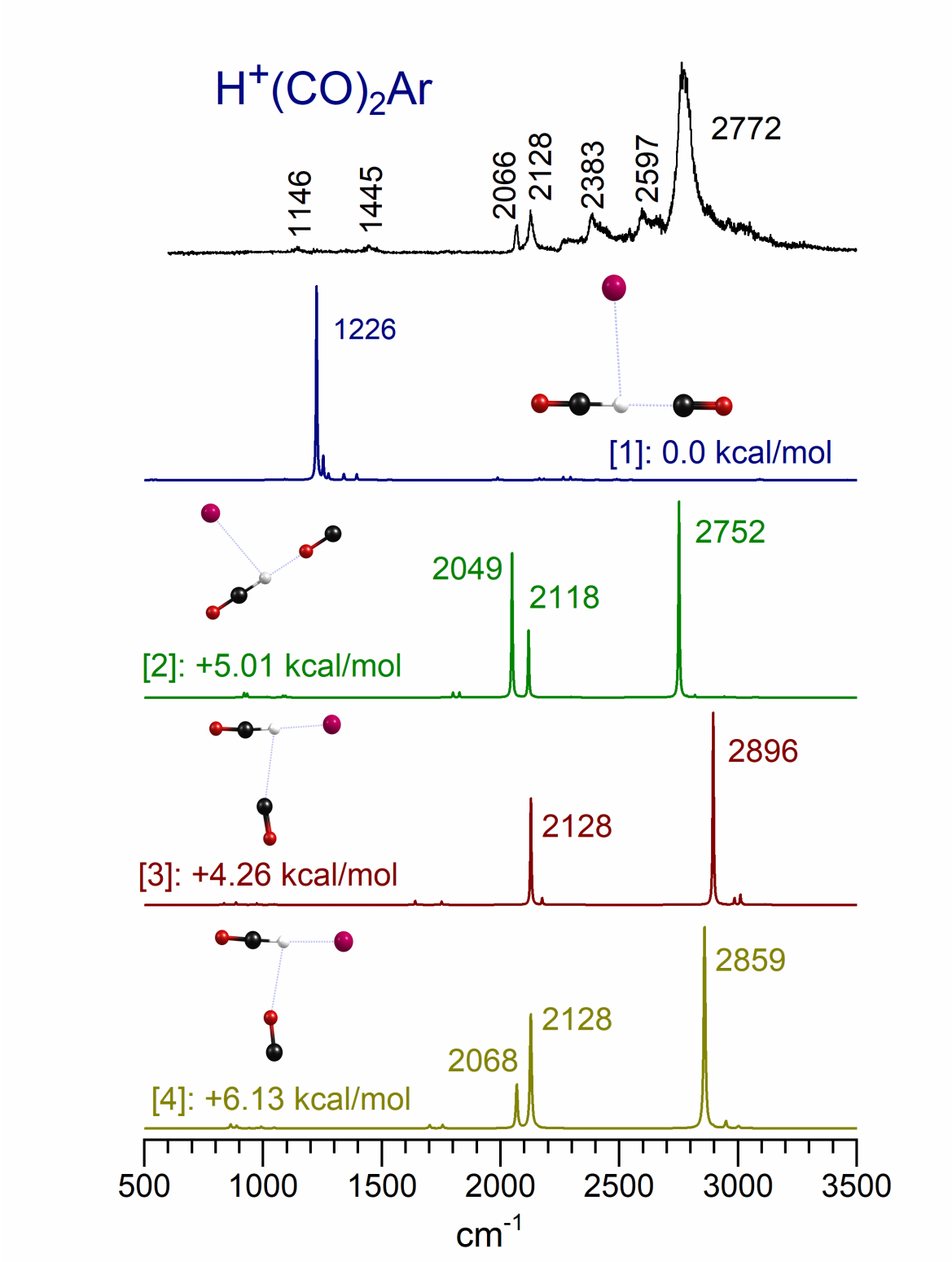
H+(CO)2Ar
1146
1445
2066
2128
2383
2597
2772
1226
[1]: 0.0 kcal/mol
2049
2118
2752
[2]: +5.01 kcal/mol
2896
2128
[3]: +4.26 kcal/mol
2859
2128
2068
[4]: +6.13 kcal/mol
500
1000
1500
2000
2500
3000
3500
cm-1

Figure 5.

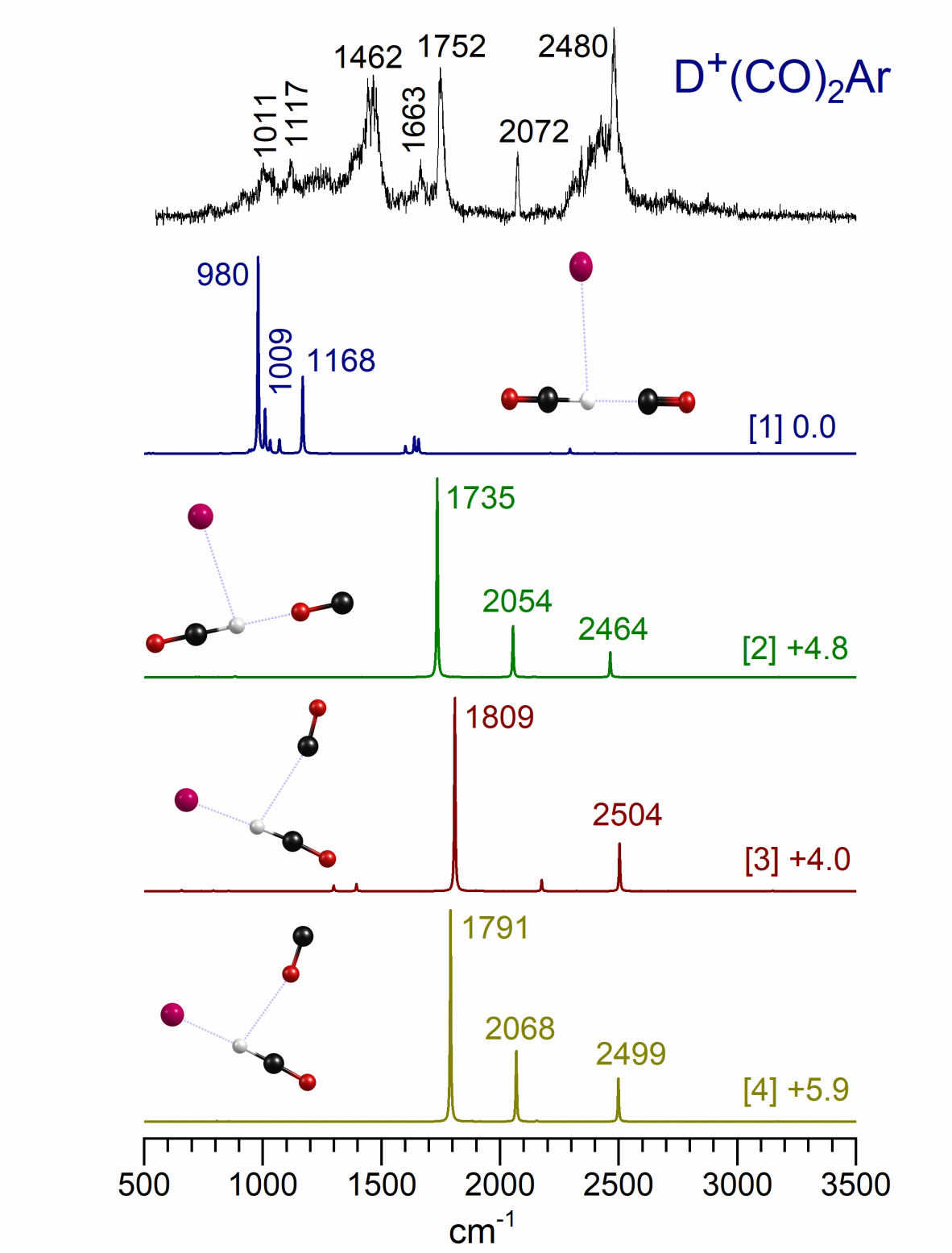
D+(CO)2Ar
1011
1117
1462
1663
1752
2072
2480
980
1009
1168
[1] 0.0
1735
2054
2464
[2] +4.8
1809
2504
[3] +4.0
1791
2068
2499
[4] +5.9
500
1000
1500
2000
2500
3000
3500
cm-1

Figure 6.

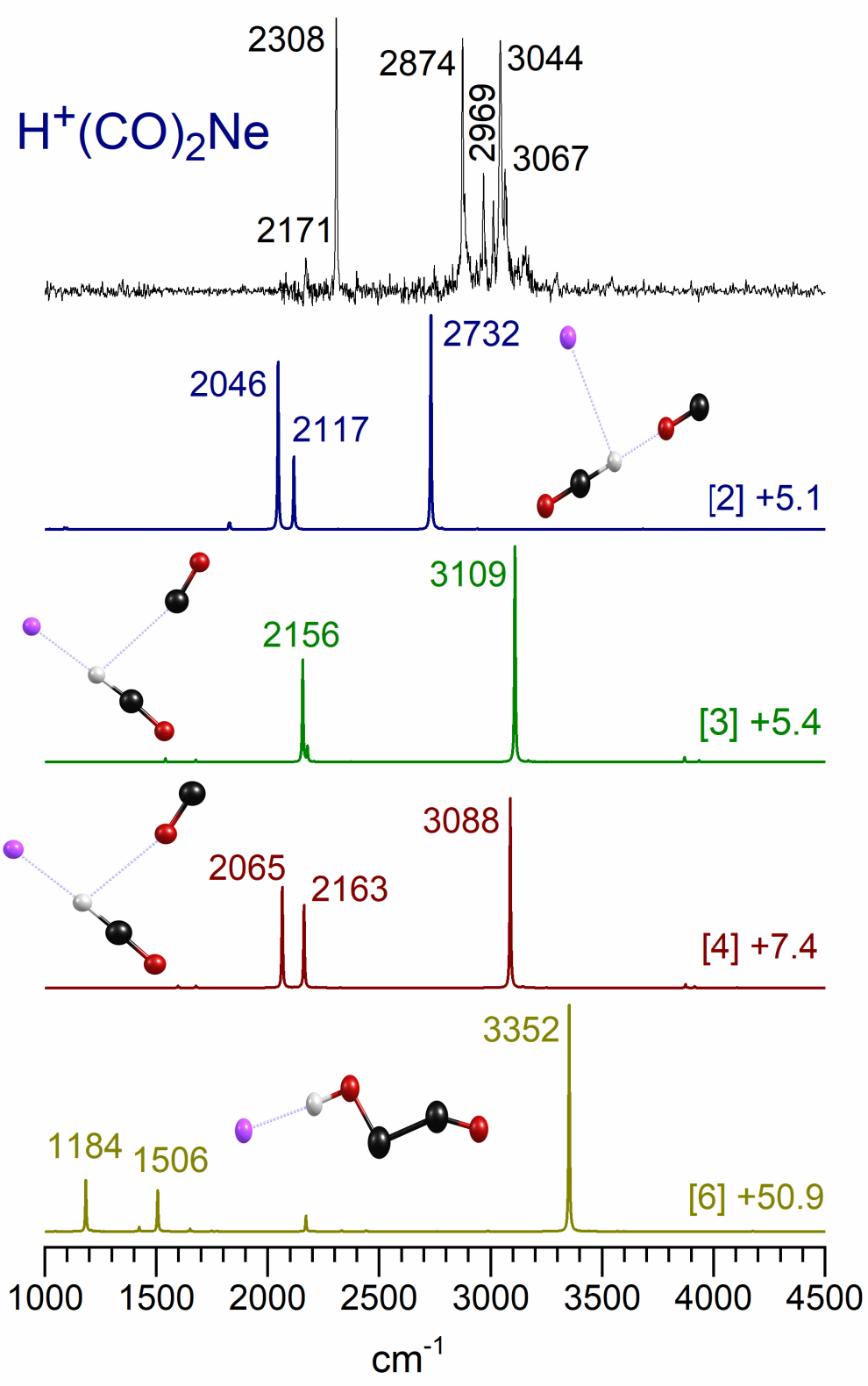
H+(CO)2Ne
2308
2874
3044
2969
3067
2171
2732
2046
2117
[2] +5.1
3109
2156
[3] +5.4
3088
2065
2163
[4] +7.4
3352
1184
1506
[6] +50.9
1000
1500
2000
2500
3000
3500
4000
4500
cm-1

Figure 7.

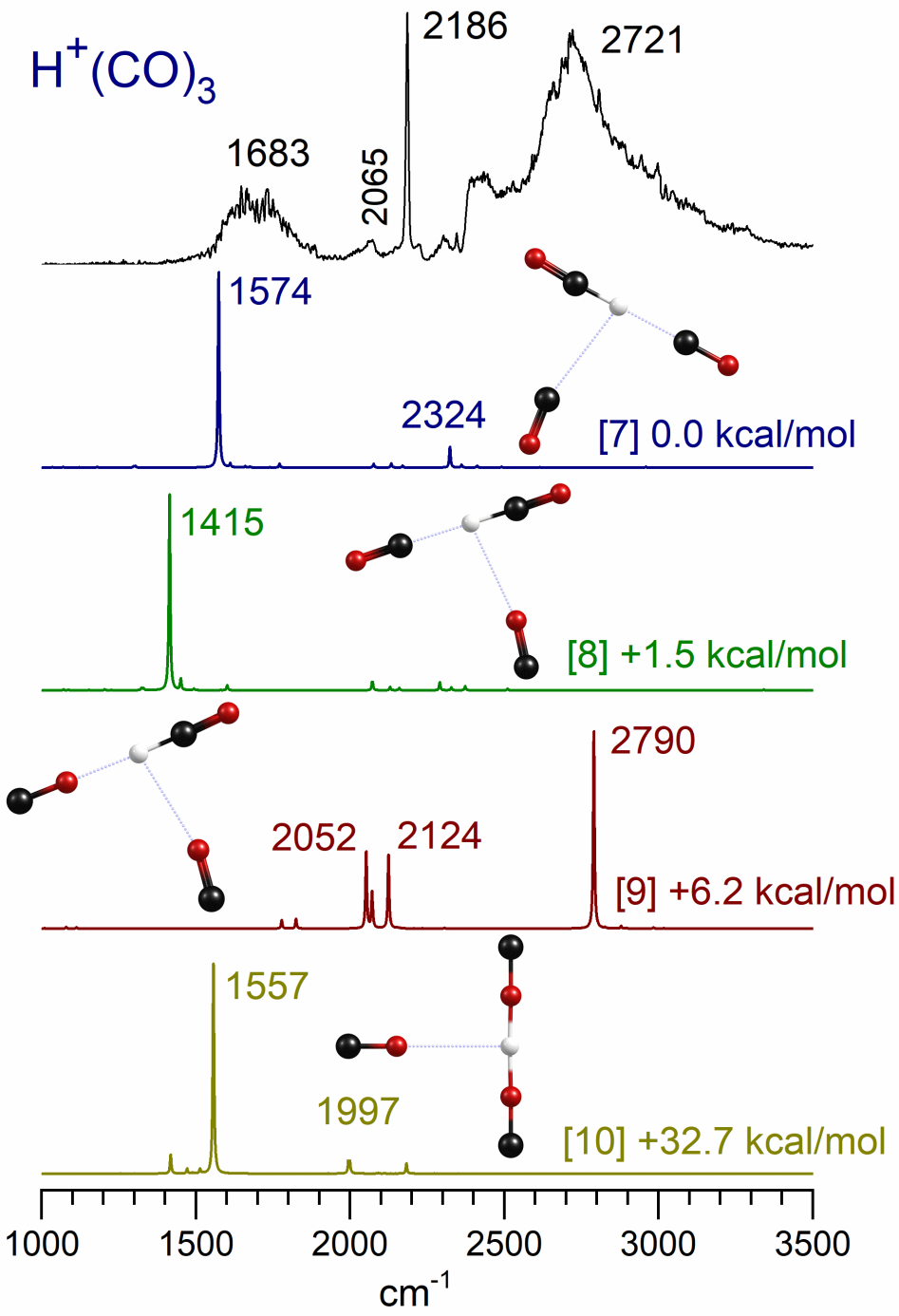
H+(CO)3
2186
2721
1683
2065
1574
2324
[7] 0.0 kcal/mol
1415
[8] +1.5 kcal/mol
2790
2052
2124
[9] +6.2 kcal/mol
1557
1997
[10] +32.7 kcal/mol
1000
1500
2000
2500
3000
3500
cm-1

Figure 8.

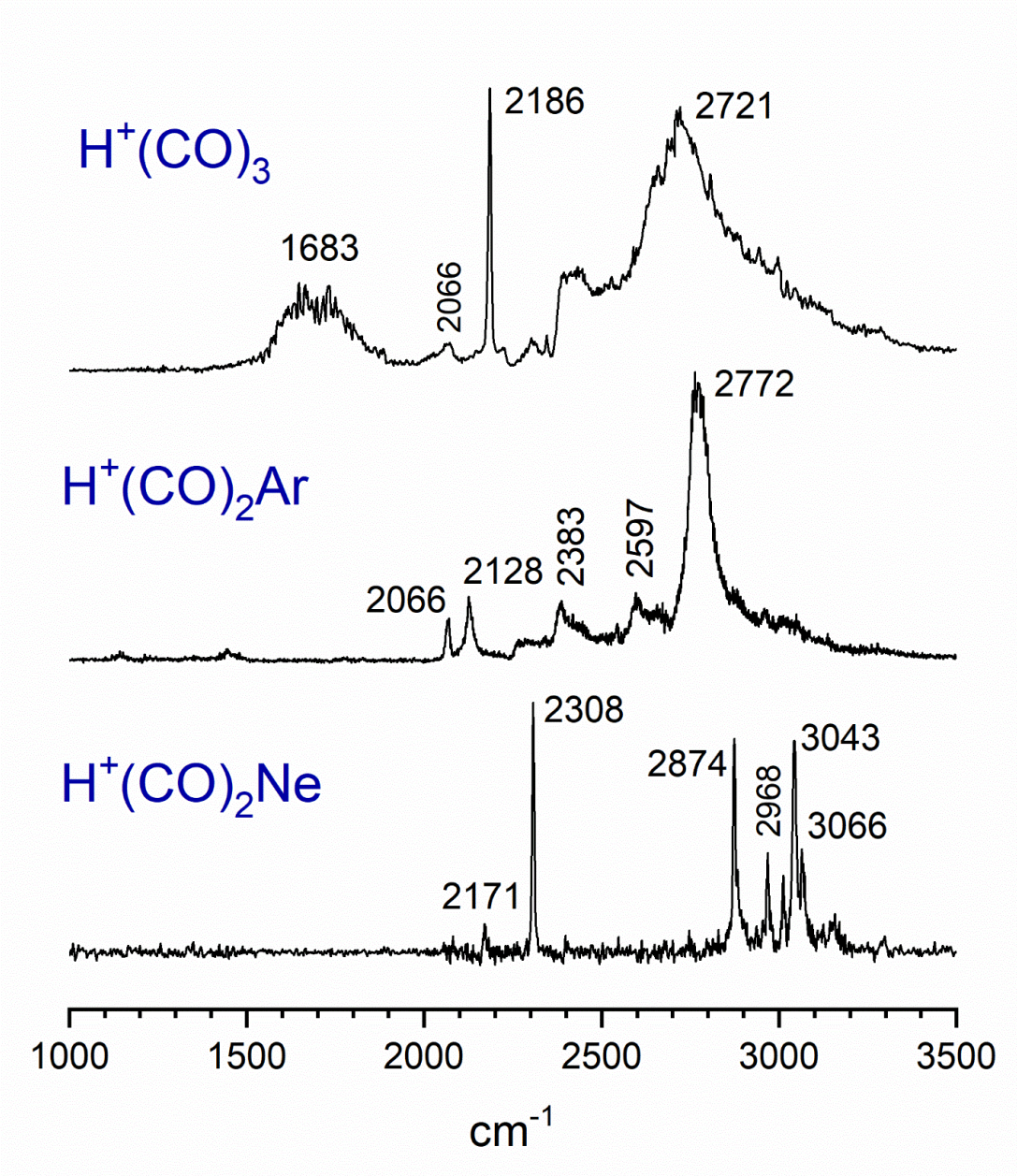
H+(CO)3
2186
2721
1683
2066
H+(CO)2Ar
2772
2066
2128
2383
2597
H+(CO)2Ne
2308
2874
3043
2968
3066
2171
1000
1500
2000
2500
3000
3500
cm-1

Figure 9.